

# Searching for tetraquark through weak decays of b-baryons



by

**Rimsha Sajjad**

**Department of Physics**

Quaid-i-Azam University Islamabad, Pakistan

(2021-2023)

A THESIS SUBMITTED IN PARTIAL FULFILLMENT OF THE REQUIREMENTS  
FOR THE DEGREE OF MASTERS OF PHILOSOPHY IN PHYSICS AT THE  
QUAID-I-AZAM UNIVERSITY, ISLAMABAD 45320, PAKISTAN. September, 2023.

## RESEARCH COMPLETION CERTIFICATE

This is to certify that Miss. Rimsha Sajjad bearing Registration No. 02182113029 has successfully completed the research work entitled "Searching for tetraquark through weak decays of b-baryons" under the supervision of Muhammad Jamil Aslam in the fulfillment of the MPhil degree.

Supervised by:

---

**Prof. M. Jamil Aslam**  
**Department of Physics**  
**Quaid-i-Azam University Islamabad**

Submitted through:

---

**Prof. Kashif Sabeeh**  
**Chairperson**  
**Department of Physics**  
**Quaid-i-Azam University Islamabad**

## **Decalaration**

I, Ms. Rimsha Sajjad Roll No. 02182113029, student of M.Phil in the subject of Physics session 2021-2023, hereby declare that the matter printed in the thesis titled “Searching for tetraquark through weak decays of b-baryons” is my review work and has not been printed, published or submitted as research work, thesis or publication in any form in any University, Research institution etc, in Pakistan.

Dated 4 September, 2023

## ACKNOWLEDGMENTS

I am thankful to Allah Almighty, who bestowed me with strength and wisdom to reach at this point where acknowledgment of thesis is being covered out. Secondly, I would like to start with my heartfelt thanks and sincere gratitude to my supervisor **Dr. M. Jamil Aslam**. Thanks for his continuous support, motivation, and enthusiasm, and for sharing his immense knowledge of the area with me in which I am so passionate. His continuous insightful comments and constructive feedback throughout my academic writing journey have been of tremendous help. Without the guidance he provided, this thesis would not have reached its current form. His intellectual insight and keen eyes for detail have helped me immensely in approaching the completion of my Mphil degree. I would like to extend my thanks to **Sudheer Muhammad, Mehmood Hassan, Talha Waseem, Anam Naz, Abdul Hafeez and Zayad Munir** for providing me with many insightful and valuable comments which contributed to shaping my research. My gratitude is also extended to **Hira Waseem** for providing me with precious academic advice and orientation. Special thanks to all the physics particle research group members. This thesis would have not come to life without their precious help and input. Thanks to my friends and colleagues, who supported me to continue my academic journey. The main thanks must go to my beloved family. Without their faith in me, my journey would not have gone so far. Thanks to my loving parent, Their words of encouragement always kept me going and inspire me all my life. Thanks to my family and friends, for giving me the strength to finish the thesis, inspiring me to go my way, and being my sparring partner at every step I take.

**Rimsha Sajjad**

# Abstract

This dissertation reviews the use of the helicity formalism for the  $\Lambda_b^0 \rightarrow \Lambda^0 Z^0(3900)$  decay to calculate the branching ratio of this process. This is an exclusive process and involve the non-perturbative quantity, i.e., the form factors. The calculation of form factors  $\Lambda_b \rightarrow \Lambda$  in helicity amplitude are studied in the full quark model wave function. We described the decay amplitudes for various processes using nonperturbative amplitudes, which parametrized in terms of the  $SU(3)$  irreducible representations. By utilizing these results, we derive several relations for the partial decay widths. These calculations allow us to estimate relevant partial decay widths of  $b$ -baryons. The outcomes reviewed in this dissertation can be experimentally tested at hadron colliders in the future. After the discovery of the charged and neutral  $Z_c(3900)$  particles, it is crucial to continue exploring different ways to produce these exotic states. In this study, we focus on investigating the potential to observe the  $Z_c(3900)$  through weak decays of  $b$ -baryons at the LHCb experiment.

# Contents

<b>1</b>	<b>Introduction</b>	<b>1</b>
<b>2</b>	<b>Standard Model</b>	<b>5</b>
2.1	Introduction . . . . .	5
2.2	Fundamental Interaction . . . . .	7
2.2.1	SM Lagrangian . . . . .	8
2.3	The CKM matrix . . . . .	14
2.4	Regularization and Renormalization . . . . .	17
2.5	Operator Product Expansion . . . . .	20
2.6	Effective Field Theory . . . . .	22
2.7	Hadrons . . . . .	27
2.8	Flavor Physics . . . . .	29
<b>3</b>	<b>Helicity Formalism of decay <math>\Lambda_b^0 \rightarrow \Lambda^0 Z_c^0</math> (3900) in SM</b>	<b>32</b>
3.1	Introduction . . . . .	32
3.1.1	Generation of Tetraquark States via Weak Decays of B-Baryons . . . . .	33
3.2	Effective Hamiltonian . . . . .	46
3.3	Helicity amplitudes and Form Factors for $\Lambda_b \rightarrow \Lambda$ transitions . . . . .	46
3.4	Kinematics of Hadronic part . . . . .	48
3.5	Hadronic Helicity amplitudes . . . . .	49
<b>4</b>	<b>Results And Discussion</b>	<b>53</b>

# Chapter 1

## Introduction

The four fundamental forces governing the basic laws of nature are the electromagnetic force, the weak force, the strong force, and gravity. These forces vary significantly in their strength, with gravity being the least powerful. However, in the current particle physics framework known as the Standard Model (SM), gravity's effects are not considered at the quantum level. The SM is defined by the gauge group  $SU(3)_C \times SU(2)_L \times U(1)_Y$ , where  $C$ ,  $L$ , and  $Y$  respectively correspond to color charge, left-handedness, and hypercharge. This model encompasses two main categories of particles: fermions, characterized by half-integer spin, and bosons, which have integer spin. Fermions can be further categorized into two families: quarks and leptons. Gauge bosons, spin-1 particles, play a role in mediating the fundamental forces as described by the SM. Additionally, the SM also includes the Higgs boson, a fundamental spin-0 particle.

The journey towards formulating the Standard Model (SM) commenced with J. J. Thomson's 1897 revelation of the electron, marking the inaugural discovery of an elementary particle. Subsequently, in 1911, Rutherford and his team detected the atomic nucleus via experiments with thin gold foil. Following this, in 1919, they pinpointed the proton. James Chadwick's 1932 identification of the neutron inaugurated the strong interaction concept, revealing a force that holds nucleons together within nuclei. The realm of particle physics emerged from cosmic ray investigations, yielding the revelation of further entities like muons, pions, kaons, and Lambda particles, categorized into "Leptons," "Mesons," and "Baryons."

Leveraging advancements in detector technology and modern accelerators, a multitude of

elementary particles were detected, a substantial portion of which proved transient. Consequently, a systematic classification system was imperative. In 1964, Gell-Mann and Zweig’s development of QCD laid the foundation for the SM model. Concurrently, experimental findings related to neutral kaons validated CP violation, consequently paving the way for electroweak theory. Independently, S. L. Glashow, A. Salam, and Steven Weinberg postulated the amalgamation of electromagnetism and the weak force in the 1960s [1]. This formulation elucidated the electroweak force and the massless nature of gauge bosons like  $\gamma$ ,  $W^+$ ,  $W^-$ , and  $Z^0$ .

The finite scope of the weak force implied that  $W$  and  $Z$  bosons were not without mass, posing a conundrum. In 1964, Brout, Englert, and Higgs introduced a mechanism conferring mass upon elementary particles, eventually clarifying this puzzle. Experimental verification of  $W$  and  $Z$  bosons materialized in 1983 at CERN. Another noteworthy triumph was the 2012 revelation of the Higgs boson, aligning with SM predictions. This particle was linked to the Higgs field and represented a fundamental spin-zero entity. Its mass was empirically determined to be  $125.09 \pm 0.21$  GeV [2]. Furthermore, the mass of the top quark was gauged at  $173.34 \pm 0.76$  GeV [3].

While the Standard Model (SM) has proven adept at explaining a substantial portion of experimental data, certain phenomena remain unaccounted for within its confines. These enigmas encompass the presence of dark matter, dark energy, neutrino oscillations, the hierarchy problem, strong CP problem, and the omission of gravitational forces from its purview. Additionally, tensions persist between SM forecasts and empirical observations in scenarios involving flavor-changing neutral current (FCNC) decays like  $b \rightarrow s\ell^+\ell^-$  and charged current  $b \rightarrow c\tau\nu$  processes. Hence, the SM is acknowledged as an unfinished framework, prompting ongoing endeavors to uncover extensions.

The pursuit of a Theory of Everything—encompassing all fundamental particles and interactions—necessitates the integration of flavor physics. This captivating field anticipated the charm quark’s existence and projected masses for both charm and top quarks even before experimental verification. It has the potential to shed light on fresh sources of CP violation, a pivotal quest given that baryogenesis implies the existence of CP violation beyond the Kobayashi-Maskawa phase depicted in the SM. Advancing beyond the SM and encom-



passing all observed phenomena mandates a search for divergences between experimental outcomes and SM projections, specifically within flavor-changing charged currents (FCCC) and flavor-changing neutral currents (FCNC) decays like  $b \rightarrow c\tau\nu$  and  $b \rightarrow s\ell^+\ell^-$ .

This quest holds promise for glimpsing New Physics (NP), a notion fortified by the SM's inadequacies in elucidating the universe's preference for matter over antimatter, neutrino mass, dark matter, dark energy, the hierarchy problem, and gravity. Furthermore, collider experiments stand as potent means to extend the theory and embrace all observed phenomena through the discovery of new particles. Flavor physics contributes indirectly by prognosticating particles through low-energy processes even before empirical detection, as exemplified by the anticipation of the  $c$ -quark,  $W$  bosons, and the  $t$ -quark mass [4].

Explorations into the decays and interactions of  $s$ ,  $c$ , and  $b$  quarks, alongside the rates and angular distributions inherent in these processes, hold the potential to furnish crucial insights into the effects exerted by NP mediators.

The discovery of the exotic state  $Z_c^\pm(3900)$  by the BESIII collaboration in 2013 posed a challenge to the traditional quark-antiquark and three-quark models of standard spectroscopy. This enigmatic state, containing a minimum of four quarks and exhibiting electric charge interaction with charmonium, offers a distinctive avenue for probing QCD. The subsequent identification of the neutral partner,  $Z_c^0(3900)$ , has intensified the intrigue surrounding these unconventional hadrons [5]. Several hypotheses have emerged, attempting to elucidate their internal quark-gluon structure and fathom the nature of the strong force. These hypotheses encompass concepts like hadroquarkonia, hadronic molecules, tetraquark states, and kinematic effects. Despite these efforts, a consensus on the inherent dynamics of these states remains elusive. Consequently, it becomes imperative to explore alternate production modes for  $Z_c(3900)$ . Recent reports from the LHCb collaboration have unveiled the existence of two additional exotic structures, designated as  $P_c(4380)$  and  $P_c(4450)$ , initially observed within the  $\Lambda_b^0 \rightarrow P_c(\rightarrow J/\psi p)K^-$  decay process [6]. Investigating weak decays of  $b$ -baryons at LHCb to uncover the  $Z_c(3900)$  could hold substantial promise. While there's no universally accepted factorization approach for handling  $Z_c$ 's production mechanisms, the application of flavor  $SU(3)$  symmetry enables us to establish correlations between decay modes in bottom-quark decays. The diquark model predicts that the charged and neutral  $Z_c(3900)$  states

may belong to the same  $SU(3)$  octet multiplet, and the discovery of other states within this multiplet would provide vital validation for this model [7].

This thesis is structured as follows: Chapter 2 offers a comprehensive review of the Standard Model (SM), encompassing its Lagrangian and the CKM matrix. The regularization and renormalization procedures are discussed in Section 2.3, while the utilization of the operator product expansion (OPE) in effective theories is presented in sections 2.4 and 2.5, respectively. An introduction to flavor physics is provided in Section 2.7. Chapter 3 revolves around a meticulous calculation of the  $\Lambda_b \rightarrow \Lambda Z(3900)$  process utilizing helicity formalism. Section 3.1 delves into the process's kinematics, followed by a detailed derivation of the amplitude.

# Chapter 2

## Standard Model

### 2.1 Introduction

The Standard Model stands as a triumphant framework in comprehending the nature of matter and its interactions. Functioning as a gauge theory, it governs the behavior of fundamental particles via quantum fields. This theoretical underpinning encapsulates all currently known elementary particle interactions, though it excludes the gravitational force. Demonstrating remarkable success, the Standard Model not only elucidates a majority of particle physics phenomena but also prognosticated the existence of particles that were then undiscovered. In accordance with its depiction, the building blocks of visible matter in the universe consist of elementary fermions, namely quarks and leptons.

Quarks and leptons, integral components of the elementary particles, are responsible for constructing the diversity of matter. A pivotal distinction lies in the fact that quarks are participants in all fundamental interactions due to their possession of color, weak, and electromagnetic charges. On the contrary, leptons do not engage in strong interaction, as they lack color charge. These divergent characteristics underscore their respective roles within the particle realm. The constituents of the Standard Model are categorized into three distinct classes, and an illustrative summary can be found in Figure 1. Below is a concise overview of the constituents comprising the Standard Model.

- • Fermions: Within the framework of the Standard Model in particle physics, there exist six distinct types of quarks, each with its own unique properties. These quark

varieties are referred to as up ( $u$ ), down ( $d$ ), charm ( $c$ ), strange ( $s$ ), top ( $t$ ), and bottom ( $b$ ) quarks. Each quark flavor is associated with a corresponding antiquark, and they all possess three different color charges. These quarks are grouped into three generations. The first generation includes up ( $u$ ) and down ( $d$ ) quarks, the second generation comprises charm ( $c$ ) and strange ( $s$ ) quarks, while the third and final generation involves top ( $t$ ) and bottom ( $b$ ) quarks. It's important to note that quarks have unique features, such as fractional electric charges, which set them apart from more familiar particles like electrons that have a charge of  $-1$ . Additionally, quarks exhibit specific properties related to their color quantum characteristics, a concept that plays a crucial role in quantum chromodynamics, the theory governing the strong nuclear force responsible for binding quarks together within particles like protons and neutrons. Up-type quarks ( $u, c, t$ ) possess an electric charge of  $+2/3$  elementary charge units, while down-type quarks ( $d, s, b$ ) carry a charge of  $-1/3$  units. The quark masses range from a few  $\text{MeV}/c^2$  to  $173 \text{ GeV}/c^2$ , as indicated in Table 1. Leptons, another category of fermions, also come in six variations: the electron, muon, tau, and their corresponding neutrinos, along with their respective antiparticles. These leptons are distributed across three generations, with each generation comprising a charged lepton ( $e^-, \mu^-, \tau^-$ ) and its neutral partner, the neutrino ( $\nu_e, \nu_\mu, \nu_\tau$ ).

- Gauge Bosons: Mediating the fundamental interactions are gauge bosons, which possess a spin of 1 and do not adhere to the Pauli Exclusion Principle. The types of gauge bosons include:
  - The photon, a neutral and massless particle, mediates the electromagnetic force.
  - The strong force is mediated by eight gluons, each with nonzero color charge and no electromagnetic charge. Gluons are also massless.
  - Weak interactions are facilitated by  $W$  and  $Z$  bosons. The  $W^\pm$  bosons, discovered at CERN in 1983, have a mass of approximately  $80.379 \pm 0.012 \text{ GeV}/c^2$  [8]. Shortly afterward, the  $Z$  boson was discovered with a mass of approximately  $91.187 \pm 0.0021 \text{ GeV}/c^2$  [9].  $W^\pm$  bosons interact primarily with left-handed particles, while the  $Z^0$

mass →	$\approx 2.3 \text{ MeV}/c^2$	$\approx 1.275 \text{ GeV}/c^2$	$\approx 173.07 \text{ GeV}/c^2$	0	$\approx 126 \text{ GeV}/c^2$
charge →	$2/3$	$2/3$	$2/3$	0	0
spin →	$1/2$	$1/2$	$1/2$	1	0
	<b>u</b> up	<b>c</b> charm	<b>t</b> top	<b>g</b> gluon	<b>H</b> Higgs boson
<b>QUARKS</b>	$\approx 4.8 \text{ MeV}/c^2$	$\approx 95 \text{ MeV}/c^2$	$\approx 4.18 \text{ GeV}/c^2$	0	
	$-1/3$	$-1/3$	$-1/3$	0	
	$1/2$	$1/2$	$1/2$	1	
	<b>d</b> down	<b>s</b> strange	<b>b</b> bottom	<b><math>\gamma</math></b> photon	
	$0.511 \text{ MeV}/c^2$	$105.7 \text{ MeV}/c^2$	$1.777 \text{ GeV}/c^2$	$91.2 \text{ GeV}/c^2$	
	-1	-1	-1	0	
	$1/2$	$1/2$	$1/2$	1	
	<b>e</b> electron	<b><math>\mu</math></b> muon	<b><math>\tau</math></b> tau	<b>Z</b> Z boson	
<b>LEPTONS</b>	$< 2.2 \text{ eV}/c^2$	$< 0.17 \text{ MeV}/c^2$	$< 15.5 \text{ MeV}/c^2$	$80.4 \text{ GeV}/c^2$	
	0	0	0	$\pm 1$	
	$1/2$	$1/2$	$1/2$	1	
	<b><math>\nu_e</math></b> electron neutrino	<b><math>\nu_\mu</math></b> muon neutrino	<b><math>\nu_\tau</math></b> tau neutrino	<b>W</b> W boson	
				<b>GAUGE BOSONS</b>	

Figure 2.1.1: Standard model[11]

boson engages both left- and right-handed particles.

- Higgs Boson: The Standard Model includes a solitary spin-0 particle known as the Higgs boson. Its discovery in 2012 at the LHC marked a significant milestone, with a measured mass of around  $125.18 \pm 0.16 \text{ GeV}/c^2$ [10]. The Higgs boson is responsible for imparting mass to all fundamental particles through the Higgs mechanism.

All the matter in the universe is made up of three fundamental particles up, down quarks and electron. The down and up quarks together form nucleons and with electron it groups up into atoms. The main goal of flavor physics is to find an answer why does Nature have not one, but three generations of matter particles and also the search for differences between matter and antimatter, as in particular it is not clear, why all the Universe seems to be made of the first generation of leptons and quarks.

## 2.2 Fundamental Interaction

The foundation of the Standard Model (SM), first proposed by Glashow, Salam, and Weinberg [13, 14], is based on the idea of preserving gauge invariance when exposed to local

symmetry group changes

$$SU(3)_C \times SU(2)_L \times U(1)_Y, \quad (2.2.1)$$

where C, L, and Y denote color charge, left-handed chirality, and weak hypercharge, respectively. The  $SU(3)_C$  gauge group is associated with strong interactions and Quantum Chromodynamics (QCD). This group possesses eight generators, corresponding to the eight gluons, which serve as the mediators of the strong force. These gluons themselves carry color charge, enabling interactions among them, leading to the phenomena of "Confinement" and "asymptotic freedom." Perturbative techniques come into play for computing color interactions, with the coupling constant  $\alpha_s$  of strong interactions becoming small at short distances and large at longer distances. This behavior gives rise to quark confinement within color-neutral hadrons like mesons and baryons.

The combined group  $SU(2)_L \times U(1)_Y$  accounts for both weak and electromagnetic interactions. The mediator for electromagnetic interaction is the massless, neutral, and colorless photon ( $\gamma$ ). Due to their lack of charge, photons do not interact with one another. As distance increases, the coupling strength of electromagnetic interactions weakens. The mediators for weak interactions are the massive  $W^\pm$  and  $Z^0$  bosons. Their mass imparts a short range to weak interactions.

In the context of the Standard Model, there exists a spin-zero particle known as the Higgs boson. Its origin traces back to the phenomenon of spontaneous symmetry breaking of  $SU(2)_L \times U(1)_Y$  into  $U(1)_{QED}$  through the non-zero vacuum expectation value (VEV) of an isospin doublet scalar Higgs field [15], denoted as

$$\phi = \begin{pmatrix} \phi^+ \\ \phi^0 \end{pmatrix} \quad (2.2.2)$$

This Higgs field encompasses four scalar degrees of freedom, three of which confer masses to the W and  $Z^0$  bosons, while the fourth manifests as the Higgs boson itself.

### 2.2.1 SM Lagrangian

The SM interaction is described by the use of total Lagrangian density, all the information contained in any theory is encoded in it. Lagrangian is the function of fields and their

derivatives containing the kinetic energy, interaction and coupling terms.

$$\mathcal{L}_{SM} = \mathcal{L}_{QCD} + \mathcal{L}_{EW} + \mathcal{L}_{Higgs} \quad (2.2.3)$$

The Lagrangian for  $SU(3)_C$  is

$$\mathcal{L}_{QCD} = -\frac{1}{4}G_{\mu\nu}^a G^{a\mu\nu} + \sum_f \bar{q}_f i \not{D} q_f, \quad (2.2.4)$$

with

$$D_\mu = \partial_\mu + ig_s G_\mu^a \frac{T^a}{2}, \quad G_{\mu\nu}^a = \partial_\mu G_\nu^a - \partial_\nu G_\mu^a - g_s f^{abc} G_\mu^b G_\nu^c, \quad (2.2.5)$$

where the covariant quark derivative is  $D_\mu$  and  $G_{\mu\nu}^a$  is the gluon field strength tensor, respectively. In Eq. (2.2.5),  $g_s$  and  $f$  in summation is for strong coupling and quark flavor, respectively and  $a, b, c = 1, \dots, 8$  are the eight-bosons of  $SU(3)_C$ . The structure constant  $f^{abc}$  are defined in terms of generators of SU(3) group

$$[T^a, T^b] = 4if^{abc}T^c \quad (2.2.6)$$

The SM combined weak and electromagnetic interaction for the electroweak sector, based on  $SU(2)_L \times U(1)_Y$  gauge symmetry group. Weinberg [16], Salam [17] and Gashow [18], developed the theory of electroweak interaction. According to this theory, the fermions comes with right-handed singlets and left-handed doublets, transform under symmetry group  $SU(2)_L \times U(1)_Y$ :

$$\Psi_L = \begin{pmatrix} \psi_L^u \\ \psi_L^d \end{pmatrix} = \begin{pmatrix} (\nu_e)_L \\ e_L \end{pmatrix}, \begin{pmatrix} (\nu_\mu)_L \\ \mu_L \end{pmatrix}, \begin{pmatrix} (\nu_\tau)_L \\ \tau_L \end{pmatrix}, \begin{pmatrix} u_L \\ d_L \end{pmatrix}, \begin{pmatrix} c_L \\ s_L \end{pmatrix}, \begin{pmatrix} t_L \\ b_L \end{pmatrix} \quad (2.2.7)$$

where,

$$\psi_r = e_r, \mu_r, \tau_r, u_r, d_r, s_r, c_r, b_r, t_r \quad (2.2.8)$$

The representations of Eq. (2.2.7) and Eq. (2.2.8) can be ordered by the quantum numbers of the weak isospin  $I$ , its third projection  $I_3$  and the weak hypercharge  $Y$ . The Gell-Mann-

Nishijima relation relate  $I_3$  and  $Y$  with electric charge  $Q$  as

$$Q = I_3 + \frac{Y}{2}, \quad (2.2.9)$$

The electroweak Lagrangian is the divided in several parts, which include the portion for the gauge boson, fermions, Higgs and Yukawa

$$\mathcal{L}_{EW} = \mathcal{L}_{gauge} + \mathcal{L}_{Higgs} + \mathcal{L}_{fermions} + \mathcal{L}_{Yukawa}. \quad (2.2.10)$$

The kinetic energy term for gauge boson read as

$$\mathcal{L}_{gauge} = -\frac{1}{4}B_{\mu\nu}B^{\mu\nu} - \frac{1}{4}W_{\mu\nu}^a W^{a\mu\nu}, \quad (2.2.11)$$

with

$$B_{\mu\nu} = \partial_\mu B_\nu - \partial_\nu B_\mu, \quad W_{\mu\nu}^a = \partial_\mu W_\nu^a - \partial_\nu W_\mu^a - g\epsilon^{abc}W_\mu^b W_\nu^c, \quad (2.2.12)$$

$B_\mu$  and  $W_\mu^a$  represent the gauge fields associated with the  $U(1)$  and  $SU(2)$  symmetry groups, respectively. 'a' can take values 1, 2, or 3, and these gauge fields correspond to the weak force's gauge bosons. The parameters 'g' and ' $\epsilon^{abc}$ ' are related to the coupling strength and the structure constant of the  $SU(2)_L$  symmetry. Initially, these bosons are considered massless, a feature dictated by the  $SU(2)_L \times U(1)_Y$  symmetry. However, they acquire mass through a process known as spontaneous symmetry breaking, specifically when the  $SU(2)_L \times U(1)_Y$  symmetry breaks down into the electromagnetic  $U(1)_{em}$  group. This mass generation mechanism is achieved through the Higgs mechanism. The Lagrangian for the Higgs part of this process can be formulated to mathematically describe how this symmetry breaking occurs.

$$\mathcal{L}_{Higgs} = (D_\mu\phi)^\dagger(D^\mu\phi) - V(\phi), \quad (2.2.13)$$

with



$$D_\mu = \partial_\mu + ig \frac{\tau^i W_\mu^i}{s} + ig' B_\mu. \quad (2.2.14)$$

Here the scalar Higgs field  $\phi$  is define in Eq. (2.2.2) with hypercharge  $+1/2$  and the term  $V(\phi)$  is the Higgs potential. The covariant derivative is  $D_\mu$  with the EM gauge coupling  $g'$  and  $\tau^i$  are the Pauli spin matrices. The square of the covariant derivative represent the three and four-point interactions between gauge bosons and the Higgs, for the spontaneous symmetry breaking the mass term should be  $\mu^2 > 0$  and  $\lambda > 0$ . Higgs potential is given as

$$V(\phi) = -\mu^2 \phi^\dagger \phi + \frac{\lambda (\phi^\dagger \phi)^2}{4}, \quad (2.2.15)$$

the potential minimization leads to  $\phi_0^\dagger \phi_0 = 2\mu^2/\lambda$ . The Higgs field doublet can be altered in the subsequent manner by selecting the smallest value of the fields.

$$\phi_0 \equiv \langle \phi_0 \rangle = 1/\sqrt{2} \begin{pmatrix} 0 \\ v \end{pmatrix}, \quad (2.2.16)$$

With 'v' representing the vacuum expectation value (VEV) defined as  $v = 2\mu/\sqrt{\lambda}$ , it's important to note that the Higgs field is a complex doublet, which means it consists of four independent components. However, through an appropriate gauge transformation, it's possible to set three out of the four components to zero. i.e., the unitary gauge:

$$\phi(x) = 1/\sqrt{2} \begin{pmatrix} 0 \\ v + h(x) \end{pmatrix}, \quad (2.2.17)$$

where the physical Higgs boson described by  $h(x)$ . The  $\tilde{\phi}$  in the unitary gauge is the charge conjugate of the Higgs field, is given as:

$$\tilde{\phi}(x) \equiv i\tau^2 \phi(x) = 1/\sqrt{2} \begin{pmatrix} v + h(x) \\ 0 \end{pmatrix}, \quad (2.2.18)$$

By using Eq (2.2.17) to the Lagrangian (2.2.13) produces the mass of  $W^\pm$  and  $Z^0$  boson,

where mass of higgs boson is  $m_h = \sqrt{2}\mu$ . Fermion interaction term in Lagrangian is

$$\mathcal{L}_{fermion} = \sum_{\Psi} \bar{\Psi}_L i \not{D} \Psi_L + \sum_{\Psi} \bar{\Psi}_R i \not{D} \Psi_R, \quad (2.2.19)$$

The summation over  $\Psi$  includes all the flavors of fermions, i.e., leptons and quarks. The  $D_\mu$  is represented as

$$(D_L)_\mu = ig \frac{\tau^i W_\mu^i}{2} + i \frac{g'}{2} Y_L B_\mu + \partial_\mu, \quad (D_R)_\mu = \partial_\mu + i \frac{g'}{2} Y_R B_\mu, \quad (2.2.20)$$

$L$  and  $R$  represent chiral projection operators, where they are defined as  $(1 \mp \gamma_5)/2$ .  $g$  is the coupling constant for the  $U(1)_Y$  group, and  $\tau^i (i = 1, 2, 3)$  are the Pauli matrices associated with the  $SU(2)_L$  group's generators, expressed as  $T^i = \tau^i/2$ . The hypercharge values  $Y_L$  and  $Y_R$  for doublets and singlets can be derived from Equation (2.2.9).

$$Y(\nu_L) = Y(e_L) = -1, \quad Y(u_L) = Y(d_L) = +\frac{1}{3}, \quad (2.2.21)$$

$$Y(e_R) = -2, \quad Y(d_R) = -\frac{2}{3}, \quad Y(u_R) = +\frac{4}{3}, \quad (2.2.22)$$

the above values holds for second and third generation for fermions. The four gauge fields  $W_\mu^i$ ,  $B_\mu$  and  $A_\mu$  represented physical fields of  $W^\pm$  and  $Z^0$  as

$$W^{\mu(*)} = (W_1^\mu \pm iW_2^\mu) / \sqrt{2}, \quad (2.2.23)$$

$$Z^\mu = c(\theta_W) W_3^\mu + s(\theta_W) B^\mu, \quad (2.2.24)$$

$$A^\mu = -s(\theta_W) W_3^\mu + c(\theta_W) B^\mu, \quad (2.2.25)$$

here  $s(\theta_W) = \sin \theta_W$  and  $c(\theta_W) = \cos \theta_W$  and  $\theta_W$  is the weak mixing angle, and can be determined as

$$c(\theta_W) = \frac{g}{\sqrt{g^2 + g'^2}} \quad (2.2.26)$$

Using the above expression of covariant derivatives and the definitions, one can obtain from

Eq. (2.2.19) the boson-fermion interaction expressions of the Lagrangian:

$$\mathcal{L}_{\psi A} = -e \sum_{\psi} Q_{\psi} (\bar{\psi} \gamma_{\mu} \psi) A^{\mu}, \quad (2.2.27)$$

$$\mathcal{L}_{\psi W} = \frac{g}{\sqrt{2}} \sum_{\psi} [(\bar{\psi}_L^d \gamma_{\mu} \psi_L^u) W^{\mu} + h.c.], \quad (2.2.28)$$

$$\mathcal{L}_{\psi Z} = \frac{g}{4 \cos \theta_W} \sum_{\psi} [\bar{\psi}^u \gamma_{\mu} (a_u - \gamma_5) \psi^u - \bar{\psi}^d \gamma_{\mu} (a_d - \gamma_5) \psi^d] Z^{\mu}, \quad (2.2.29)$$

where

$$a_u = 1 - 4Q_u \sin^2 \theta_W, \quad (2.2.30)$$

$$a_d = 1 + 4Q_d \sin^2 \theta_W \quad (2.2.31)$$

and the electromagnetic charge  $e$  is

$$e = \frac{gg'}{\sqrt{g^2 + g'^2}} = g \sin(\theta_W) = g' \cos(\theta_W). \quad (2.2.32)$$

The way that left and right-handed fields transform in different manner leads to parity violation in the electroweak interaction. In the SM Lagrangian for Yukawa interaction is split into two section

$$\mathcal{L}_{Yukawa} = \mathcal{L}_Y^{leptons} + \mathcal{L}_Y^{quarks}. \quad (2.2.33)$$

The Yukawa interaction for the lepton with Higgs boson is

$$\mathcal{L}_Y^{leptons} = -Y_{ij}^{(l)} (\bar{L}_L^i \phi) l_R^j + h.c. \quad (2.2.34)$$

$L_L^i$  is a doublet containing left-handed leptons, where  $l^i$  represents different lepton flavors ( $e, \mu, \tau$ ).  $l_R^i$  represents the right-handed lepton singlet.  $\phi$  represents the Higgs doublet defined in Equation (2.2.2).  $Y_{ij}^{(l)}$  is a  $3 \times 3$  matrix describing the Yukawa coupling between leptons, and it's a diagonal matrix denoted as  $Y_{ij}^{(l)} = \delta_{ij} * Y_{ii}^{(l)}$ . This diagonal structure arises because lepton number conservation is maintained, and lepton mixing is not considered in the Standard Model. The right-handed neutrinos is not present in Eq. (2.2.22) as in SM framework

neutrinos are massless.

## 2.3 The CKM matrix

Quark mixing comes about as a result of the Yukawa interaction between quark and Higgs fields. Within the framework of the Standard Model (SM), the Charge Conjugation-parity (CP) symmetry is preserved for the kinetic energy component of quarks, leptons, and the Higgs doublet. CP violation emerges from interaction terms, often mediated through Yukawa couplings. When the Vacuum Expectation Value (VEV) of the Higgs doublet is zero, CP violation does not occur. Beneath the VEV scale of the Higgs doublet, SM fields acquire masses, and CP phases are typically found in the left-handed currents that couple with the  $W_\mu^\pm$  bosons. Within this arrangement, the couplings of charged currents are defined using the Cabbibo-Kobayashi-Maskawa (CKM) matrix for quarks [19]. The Yukawa interaction is characterized by the Lagrangian, which is as follows:

$$\mathcal{L}_Y^{quarks} = -Y_{ij}^{(d)} (\bar{Q}_L^i \phi) d_R^j - Y_{ij}^{(u)} (\bar{Q}_L^i \tilde{\phi}) u_R^j + h.c. \quad (2.3.1)$$

we have the  $SU(2)$  left-handed doublet of quark fields represented by  $u^i (i = u, c, t)$  and  $d^i (i = d, s, b)$  within the  $Q_L^i$  doublet. Additionally, there are up-type quark singlets  $u_R^j$  and down-type quark singlets  $d_R^j$ . The Higgs fields, both the doublet  $\varphi$  and its conjugate, denoted as  $\varphi^c$ , are defined as described in Equations (2.2.17) and (2.2.18). The matrices  $Y(u)$  and  $Y(d)$  are 3x3 complex matrices representing the Yukawa couplings for up-type and down-type quarks, respectively. Mass terms are generated by substituting  $\varphi(x)$  with its vacuum expectation value (VEV),  $\varphi \rightarrow \langle \varphi \rangle$ , as outlined in Equation (2.2.16).

$$\mathcal{L}_Y^{quark} \rightarrow \mathcal{L}_Y^{quark} = -\frac{v}{\sqrt{2}} Y_{ij}^{(d)} \bar{d}_L^i \bar{d}_R^j - \frac{v}{\sqrt{2}} Y_{ij}^{(u)} \bar{u}_L^i \bar{u}_R^j + h.c. \quad (2.3.2)$$

The bilinear term involving quark fields in Equation (2.3.2) can be made diagonal by using four unitary 3x3 matrices, denoted as  $V_L^u, V_R^u$  for up-type quarks, and  $V_L^d, V_R^d$  for down-type

quarks. This diagonalization process results in the emergence of mass eigenstates.

$$[\tilde{u}_{L,R}]^i = [V_{L,R}^u]^{ij} [u_{L,R}]^j, \quad [\tilde{d}_{L,R}]^i = [V_{L,R}^d]^{ij} [d_{L,R}]^j, \quad (2.3.3)$$

and the diagonal mass matrices

$$M_q = \frac{v}{\sqrt{2}} V_L^q Y^{(q)} V_R^{q\dagger}, \quad q = u, d. \quad (2.3.4)$$

The process of transforming quarks into their mass eigenstates, as outlined in Equation (2.3.3), preserves the diagonal components in the Lagrangian. This encompasses both the kinetic terms and interaction terms involving neutral bosons, as presented in Equations (2.2.27) and (2.2.29), respectively. The unitary nature of these transformations ensures this preservation. The only change is encountered when dealing with the interaction between charged W-bosons and quark fields, as specified in Equation (2.2.28). This modification results in the multiplication of unitary matrices. The  $3 \times 3$  unitary matrix  $V_{CKM}$ , governing quark transitions while generating a virtual W-boson, can be expressed as follows:

$$V_L^u V_L^{d\dagger} \equiv V_{CKM} = \begin{pmatrix} V_{ud} & V_{us} & V_{ub} \\ V_{cd} & V_{cs} & V_{cb} \\ V_{td} & V_{ts} & V_{tb} \end{pmatrix} \quad (2.3.5)$$

The following formula may be used to represent the Lagrangian of the relationship between the W-boson and the quark mass eigenstates:

$$\mathcal{L}_{Wq} = \frac{g}{\sqrt{2}} (\bar{u}_L, \bar{c}_L, \bar{t}_L) \gamma^\mu V_{CKM} \begin{pmatrix} d_L \\ s_L \\ b_L \end{pmatrix} W_\mu^\dagger + h.c. \quad (2.3.6)$$

The Lagrangian in Eq. (2.3.6) allows the flavor-changing transition between different generations of quarks, i.e.,  $b \rightarrow u$ . The ability to alter quark flavors in weak interactions is highly significant because it enables the decay of b-quarks into lighter quarks like u, d, s, and c. This characteristic leads to a wide range of possible decay processes for B mesons that

contain b-quarks.. The  $V_{CKM}$  has many possible conventions, however a standard one is

$$V_{CKM} = \begin{pmatrix} c_{12}c_{13} & s_{12}c_{13} & s_{13}e^{-i\delta} \\ -s_{12}c_{23} - c_{12}s_{23}s_{13}e^{i\delta} & c_{12}c_{23} - s_{12}s_{23}s_{13}e^{i\delta} & s_{23}c_{13} \\ s_{12}s_{23} - c_{12}c_{23}s_{13}e^{i\delta} & -c_{12}s_{23} - s_{12}c_{23}s_{13}e^{i\delta} & c_{23}c_{13} \end{pmatrix}, \quad (2.3.7)$$

where  $s_{ij} = \sin(\theta_{ij})$ ,  $c_{ij} = \cos(\theta_{ij})$  and the phase  $\delta$  is responsible for the CP violation [20]. All  $\theta_{ij}$  lie in 1<sup>st</sup> quadrant and it is experimentally verified that  $s_{13} \ll s_{23} \ll s_{12} \ll 1$ . To demonstrate this hierarchy, it was deemed helpful to express the CKM matrix using four parameters:  $A$ ,  $\lambda$ ,  $\rho$ , and  $\eta$  as [21]

$$s_{12} = \lambda = \frac{|V_{us}|}{\sqrt{|V_{ud}|^2 + |V_{us}|^2}}, \quad (2.3.8)$$

$$s_{23} = A\lambda^2 = \lambda \frac{|V_{cb}|}{|V_{us}|}, \quad (2.3.9)$$

$$s_{13}e^{i\delta} = V_{ub}^* = A\lambda^3(\rho + i\eta), \quad (2.3.10)$$

Here,  $\lambda$  is a small parameter, and when expanded to the order of  $\lambda^4$ , the CKM matrix can be formulated as

$$V_{CKM} = \begin{pmatrix} 1 - \frac{\lambda^2}{2} & \lambda & A\lambda^3(\rho - i\eta) \\ -\lambda & 1 - \frac{\lambda^2}{2} & A\lambda^2 \\ A\lambda^3(1 - \rho - i\eta) & -A\lambda^2 & 1 \end{pmatrix} + \mathcal{O}(\lambda^4). \quad (2.3.11)$$

Additionally, one defines  $\bar{\rho} + i\bar{\eta} = -(V_{ud}V_{ub}^*) / (V_{cd}V_{cb}^*)$ , where parameters  $\bar{\rho}$  and  $\bar{\eta}$  are related with  $\rho$  and  $\eta$  as

$$\bar{\rho} = \rho \left( 1 - \frac{\lambda^2}{2} + \mathcal{O}(\lambda^4) \right), \quad (2.3.12)$$

$$\bar{\eta} = \eta \left( 1 - \frac{\lambda^2}{2} + \mathcal{O}(\lambda^4) \right). \quad (2.3.13)$$

The CKM matrix unitarity gives ( $VV^\dagger = V^\dagger V = I$ )

$$\sum_k V_{ik}V_{jk}^* = \delta_{ij} \quad \text{and} \quad \sum_k V_{kj}V_{ki}^* = \delta_{ij}, \quad (2.3.14)$$

yielding in the particular the commonly used constraint

$$V_{ud}V_{ub}^* + V_{cd}V_{cb}^* + V_{td}V_{tb}^* = 0 \quad (2.3.15)$$

From the relevant decays, CKM matrix elements  $V_{ij}$  the values can be extracted from the experimental data.

## 2.4 Regularization and Renormalization

Equation (4), representing the QCD Lagrangian density, offers a means to compute the amplitude of a process within perturbative QCD. Nonetheless, at the tree level, the self-interaction among particles can lead to ultraviolet divergences, introducing the challenge of infinite values. Tackling these ultraviolet infinities stands as one of the most intricate hurdles in relativistic quantum field theory. The resolution of these issues has only been systematically achieved in Quantum Electrodynamics (QED), wherein infinities are consistently absorbed into the bare quantities, rendering a physically meaningful outcome.

To remove these divergences and achieve physically interpretable results, a technique called renormalization comes into play. This involves employing a regularization process to modify the theory in such a way that observables like mass and charge remain well-defined and finite across all orders in perturbation theory. Two primary methods for applying the regularization scheme are the momentum cut-off and dimensional regularization.

The momentum cut-off approach, while preserving all gauge symmetries and Ward identities, violates Lorentz invariance [22]. In contrast, the dimensional regularization method maintains gauge symmetries and Ward identities to all orders of perturbation theory, ensuring a more consistent treatment of the theory. The cut-off regularization, introduced to regulate field theory, effectively sets an energy scale. By assigning a finite value to the cut-off, initially divergent integrals are transformed into convergent ones, albeit with a cut-off dependence. However, these terms cancel out with their cut-off counterparts, ultimately yielding finite physical results when the cut-off is allowed to approach infinity.

Remarkably, even in cases where loop diagrams do not exhibit divergence in a quantum

field theory, the renormalization of mass and fields remains necessary. This arises from the presence of a cloud of virtual particles surrounding a system of charged particles, which leads to alterations in the original parameters that define the system, such as its mass and charge.

$$m^{(0)} = Z_m m, \quad q^{(0)} = Z_q^{\frac{1}{2}} q, \quad g^{(0)} = Z_g g \mu^\epsilon, \quad A_\mu^{(0)} = Z_3^{\frac{1}{2}} A_\mu. \quad (2.4.1)$$

Here the quantities with superscript (0) are bare and  $m, q, g$  and  $A_\mu$  are renormalized quark mass, charge, QCD coupling and photon field, respectively.  $Z_m, Z_q, Z_g$  and  $Z_3$  are the renormalized constants in which all divergence are absorbed up to all powers of perturbation. A simplified method to apply renormalization is a counter-term method, where QCD bare Lagrangian  $\mathcal{L}_{QCD}^{(0)}$  can be written as

$$\mathcal{L}_{QCD}^{(0)} = \mathcal{L}_{QCD} + \mathcal{L}_{counter}, \quad (2.4.2)$$

with  $\mathcal{L}_{QCD}$  given by Eq. (2.2.4) and the term  $\mathcal{L}_{counter}$  term is proportional to  $(Z - 1)$  that acts as new interaction term contributing to Green's functions in the perturbation theory. Renormalization constants  $Z_{m,q,g,3}$  are fixed in such a way that this new term cancel the contributions of divergence in Green's functions. But a sensible scheme for this cancellation must be defined otherwise convergent terms are also canceled out along with divergent ones. The two scheme designed for this purpose an  $MS$  and  $\overline{MS}$ , where the  $\overline{MS}$  scheme is one of prime interest in which renormalization scale  $\mu$  reads as

$$\mu_{\overline{MS}} \rightarrow \frac{\mu e^{\gamma_E/2}}{\sqrt{4\pi}}. \quad (2.4.3)$$

This scheme is used to proceed so that in  $4\pi - \gamma_E$  terms are no more present and not only the divergent part of radiative corrections is removed by counter terms but also the universal constant appeared in Feynman diagram calculations. In this scheme renormalization constants take the from

$$Z_m = 1 - 3C_F \frac{\alpha_s}{4\pi\epsilon}, \quad Z_g = 1 - \frac{\alpha_s}{4\pi\epsilon} \left( \frac{11}{6} N_c - \frac{1}{3} N_f \right), \quad (2.4.4)$$



$$Z_q = 1 - C_F \frac{\alpha_s}{4\pi\epsilon}, \quad Z_3 = 1 - \frac{\alpha_s}{4\pi\epsilon} \left( \frac{2}{3}N_c - \frac{5}{3}N_f \right), \quad (2.4.5)$$

where  $N_c$  and  $N_f$  are colors and flavors of quarks, respectively. Now the parameters of theory depend on renormalization scale  $\mu$  and it must be assigned a certain value to get renormalized parameters from experiment; i.e.,  $g = g(\mu)$ ,  $m = m(\mu)$ , and  $q = q(\mu)$ . By varying the value of  $\mu$ , one can get different sets of parameters of theory  $m(\mu)$ ,  $q(\mu)$ ,  $g(\mu)$  along with a set of equations, which relates parameter set with different values of  $\mu$  and these are called the renormalization group equations (RGE). Using Eq. (2.4.1) one can get

$$\frac{dm(\mu)}{d\ln(\mu)} = -m(\mu)\gamma_m(g(\mu)), \quad \frac{dg(\mu)}{d\ln(\mu)} = \beta(g(\mu, \epsilon)), \quad (2.4.6)$$

where anomalous dimension of mass operator and  $\beta$  function are define as

$$\gamma_m(g(\mu)) = \frac{1}{Z_m} \frac{dZ_m}{d\ln(\mu)}, \quad \beta(g(\mu, \epsilon)) = -\epsilon g + \beta(g), \quad (2.4.7)$$

with

$$\beta(g) = -\frac{1}{Z_g} \frac{dZ_g}{d\ln(\mu)}. \quad (2.4.8)$$

Up to two loop accuracy one gets

$$\gamma_m(\alpha_s) = \frac{\alpha_s}{4\pi}\gamma_m^{(0)} + \left(\frac{\alpha_s}{4\pi}\right)^2\gamma_m^{(1)}, \quad \beta(g) = -\frac{g^3}{16\pi^2}\beta_0 - \frac{g^5}{(16\pi^2)^2}\beta_1, \quad (2.4.9)$$

where

$$\begin{aligned} \gamma_m^{(0)} &= 6C_F, & \gamma_m^{(1)} &= C_F(3C_F + \frac{97}{3}N_c - \frac{10}{3}N_f), \\ \beta_0 &= \frac{11N_c - 2N_f}{3} & \beta_1 &= \frac{34}{3}N_c^2 - \frac{10}{3}N_cN_f - 2C_FN_f, \\ \alpha_s(\mu) &= \frac{g^2(\mu)}{4\pi}, & C_F &= \frac{N_c^2 - 1}{2N_c}. \end{aligned} \quad (2.4.10)$$

One gets the solutions for  $m(\mu)$  and  $\alpha_s(\mu)$  as

$$m(\mu) = m(\mu_0) \left[ \frac{\alpha_s(\mu)}{\alpha_s(\mu_0)} \right]^{\frac{\gamma_m^{(0)}}{2\beta_0}} \left[ 1 + \left( \frac{\gamma_m^{(1)}}{2\beta_0} - \frac{\beta_1\gamma_m^{(0)}}{2\beta_0^2} \right) \frac{\alpha_s(\mu) - \alpha_s(\mu_0)}{4\pi} \right], \quad (2.4.11)$$

$$\alpha_s(\mu) = \frac{4\pi}{\beta_0 \ln\left(\frac{\mu^2}{\Lambda_{\overline{MS}}^2}\right)} \left[ 1 - \frac{\beta_1}{\beta_0^2} \frac{\ln\left(\ln\left(\frac{\mu^2}{\Lambda_{\overline{MS}}^2}\right)\right)}{\ln\left(\frac{\mu^2}{\Lambda_{\overline{MS}}^2}\right)} \right]. \quad (2.4.12)$$

The cut-off  $\Lambda_{\overline{MS}}$  is a characteristics scale both for QCD and the used  $\overline{MS}$  scheme and depends on the quark flavors present in the  $\beta_0$  and  $\beta_1$ .  $\beta_0$  and  $\gamma_m^{(0)}$  are positive for six quark flavor and three colors, which leads to the phenomenon of asymptotic freedom because coupling (also mass) decrease as  $\mu$  increase. Renormalization group has its advantages when we want to sum large logarithms such as the one present in  $\alpha_s$  given in Eq. (2.4.12) which can be represent in the form

$$\alpha_s(\mu) = \frac{\alpha_s(\mu_0)}{v(\mu)} \left[ 1 - \frac{\beta_1}{\beta_0} \frac{\alpha_s(\mu)}{4\pi} \frac{\ln v(\mu)}{v(\mu)} \right], \quad (2.4.13)$$

where  $v(\mu) = 1 - \beta_0 \frac{\alpha_s}{4\pi} \ln \frac{\mu^2}{\mu_0^2}$ .

## 2.5 Operator Product Expansion

The dimensional regularization method, as discussed in Section 2.3, often encounters logarithmic terms involving ratios of scales to the renormalization scale  $\mu$ . These substantial logarithms can be systematically summed using Renormalization Group Equations (RGEs). However, challenges arise when considering energy scales around 1 GeV, particularly within the realm of hadronic energy scales. In addition to these significant logarithmic terms, the strong coupling constant  $\alpha_s$  becomes too large for traditional perturbation theory to be applicable. This necessitates the development of a theoretical framework capable of describing the weak interaction of quarks. A robust approach to address this challenge involves the utilization of a well-established tool known as the Operator Product Expansion (OPE) [25].

The OPE can be explained using an example of a quark level  $b \rightarrow cs\bar{u}$  transition with an amplitude

$$\begin{aligned} A(b \rightarrow cs\bar{u}) &= -\frac{G_F}{\sqrt{2}} V_{cb} V_{us}^* \frac{M_W^2}{p^2 - M_W^2} [\bar{s}\gamma_\alpha(1 - \gamma^5)u] [\bar{c}\gamma^\alpha(1 - \gamma^5)u], \\ &= \frac{G_F}{\sqrt{2}} V_{cb} V_{us}^* [\bar{s}\gamma_\alpha(1 - \gamma^5)u] [\bar{c}\gamma^\alpha(1 - \gamma^5)u] + \mathcal{O}\left(\frac{p^2}{M_W^2}\right), \end{aligned} \quad (2.5.1)$$

where  $W$ -boson propagate the process and  $q_1\gamma_\mu(1 - \gamma_5)q_2$  is the axial-vector currents. As

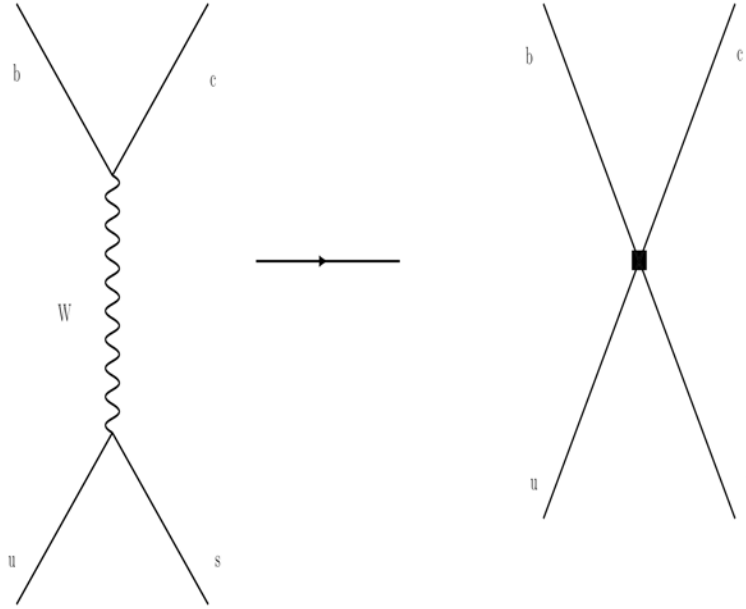


Figure 2.5.1: Feynman diagram for the decay  $b \rightarrow cs\bar{u}$  which can be replaced by four point effective vertex.

momentum transfer  $p$  is significantly less than  $M_W$  therefore, one can safely ignore the terms of order  $\frac{p^2}{M_W^2}$  and the problem can be tackled by replacing the propagator with a four point fermion interaction as shown in Fig. 2.5.1

The OPE in quantum field theory is a convergent expansion obtained from the product of two fields lying at different point as a sum of local operators. Consider a state  $\Psi$  that is characterized by  $N$  point functions

$$\langle \mathcal{O}^{A_1}(x_1), \dots, \mathcal{O}^{A_N}(x_N) \rangle \Psi = \sum_B C_B^{A_1, \dots, A_N}(x_1, \dots, x_N) \langle \mathcal{O}_B(x_N) \rangle \Psi,$$

where  $C_B^{A_1, \dots, A_N}(x_1, \dots, x_N)$  are the OPE coefficients that are independent of  $\Psi$  and covariant functional of metric tensor  $g_{\mu\nu}$ . For four dimensional free scalar field having action  $\int |\partial\phi|^2$ , the OPE reads

$$\phi(x_1)\phi(x_2) = \frac{\lambda}{|x_1 - x_2|^2} + \phi^2(x_2) + \sum \frac{(x_1 - x_2)^{\mu_1} \dots (x_1 - x_2)^{\mu_N}}{N!} \phi \partial_{\mu_1, \dots, \mu_N} \phi(x_2), \quad (2.5.2)$$

where  $\frac{\lambda}{|x_1 - x_2|^2} = C_{AB}^C$  and for  $\mathcal{O}_A = \mathcal{O}_B = \phi$  then  $\mathcal{O}_C = 1$ .

## 2.6 Effective Field Theory

The effective theory approach stands as a crucial method for investigating theories encompassing diverse energy scales. When various scales come into play, calculating decay amplitudes using the complete theory's Lagrangian becomes intricate due to the presence of significant logarithms like  $\ln\left(\frac{m_W}{\Lambda_{QCD}}\right)$  causing perturbation theory to break down. Specifically, when dealing with processes occurring at energies below the masses of heavy quarks such as charm, bottom, and top (with masses 1.4 GeV, 4.8 GeV, and 175 GeV respectively), it proves advantageous to establish an effective theory. This involves integrating out the degrees of freedom associated with heavy quarks from the Lagrangian of the comprehensive theory. This simplification streamlines analysis and facilitates the extraction of relevant outcomes.

Exploring weak decays of hadrons necessitates a meticulous consideration of strong interactions. Flavor-changing weak interactions are governed by the electroweak scale, fixed at  $m_W=80$  GeV. In contrast, the strong interactions governing the fundamental forces of final hadronic states operate at the scale  $\Lambda_{QCD} = 0.2\text{GeV}$  (associated with non-perturbative QCD). The b-quark mass, lying between the weak and QCD scales, characterizes intermediate states.

To manage Flavor-Changing Neutral Current (FCNC) interactions, dimension-six operators are introduced in the theory, involving gluons, photons, quarks excluding the top quark, and leptons. These operators are influenced by Wilson Coefficients (WCs). The QCD corrections to weak processes can be computed through a perturbative approach. It is anticipated that newly added fields within the theory would possess masses surpassing that of the b-quark, and New Physics (NP) could enter the theory by introducing new operators or modifying existing Wilson Coefficients.

Effective theory can be obtained by adopting following steps :

1. Select a cutoff scale  $\Lambda$  and split the field  $\phi$  in high and low energy components  $\phi_H$  and  $\phi_L$ , respectively; i.e.,  $\phi = \phi_H + \phi_L$ . Low energy mode  $\phi_L$  can be written as

$$\langle 0 | T(\phi_L(x_1) \dots \phi_L(x_n)) | 0 \rangle = \frac{1}{Z[0]} \left( -\frac{i\delta}{\delta j_L(x_1)} \right) \dots \left( -\frac{i\delta}{\delta j_L(x_n)} \right) Z[j_L] |_{j_L=0}, \quad (2.6.1)$$

with the generating functional

$$Z[j_L] = \int \mathcal{D}\phi_L \mathcal{D}\phi_H e^{i \int d^d x \mathcal{L}(x) + i \int d^d x j_L(x) \phi_L(x)}. \quad (2.6.2)$$

2. Integrate high energy modes above the scale  $\Lambda$

$$Z[j_L] = \int \mathcal{D}\phi_L \left( \int \mathcal{D}\phi_H e^{i \int d^d x \mathcal{L}(x)} \right) e^{i \int d^d x j_L(x) \phi_L(x)}, \quad (2.6.3)$$

where  $\int \mathcal{D}\phi_H e^{i \int d^d x \mathcal{L}(x)}$  is called the Wilsonian effective action, which is non-local at  $\Delta x^\mu \sim 1/\Lambda$  is dependent on the selection of cutoff  $\Lambda$ . After integrating on  $\phi_H$ , Eq. (2.6.2) is independent of fields  $\phi_H$  for which  $E > \Lambda$ .

3. Apply OPE on non-local action in low energy regime to expand it in terms of non-local operators comprising of fields for which  $E \ll \Lambda$

$$S_\Lambda(\phi_L) = \int d^d x \mathcal{L}_\Lambda^{eff}(x), \quad (2.6.4)$$

where

$$\mathcal{L}_\Lambda^{eff}(x) = \sum_i c_i \mathcal{O}_i(\phi_L(x)). \quad (2.6.5)$$

The above procedure allows us to get the Lagrangian corresponding to specific scale.

The matrix elements do not involve perturbative QCD, where as the WC's are calculated in perturbation theory at a weak scale  $\mu_o = m_W$ . The WC's are evaluated using Feynman diagrams of Fig. 2.6.1 and then matching the computed results onto the effective theory. The matched calculation fix the initial conditions at high scale  $\sim \mu_{W,t}$ .

The RGE

$$\frac{d}{d \ln \mu} C_i(\mu) = \gamma_{ji}(\mu) C_j(\mu), \quad (2.6.6)$$

is solved which defines the mixing of operators and the evolution at a low scale. In Eq. (2.6.6) anomalous dimension matrix is define as

$$\gamma_{ji}(\mu) = Z_{ik}^{-1} \frac{dZ_{kj}}{d \ln \mu}. \quad (2.6.7)$$

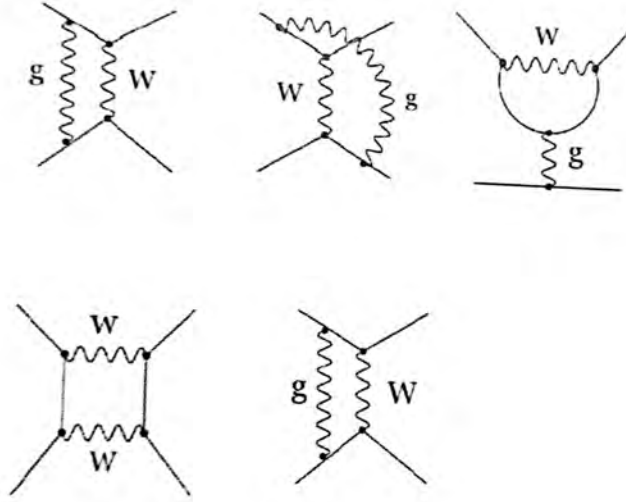


Figure 2.6.1: The quark level transition Feynman diagram in full theory.

It can expand in terms of power of strong coupling  $\alpha_s(\mu)$ . The initial conditions are known at next-to-leading order (NLO) for electroweak interaction and next-to-next-to-leading order (NNLO) for QCD for all the WC's. To solve Eq. (2.6.6), the procedure follow in section 2.3 can be used. It seems straight forward to leading accuracy but quite difficult beyond the leading order as perturbation expansion for  $\gamma_{ij}$  gives

$$\gamma_{ij} = \gamma_{ij}^{(0)} \frac{\alpha_s}{4\pi} + \gamma_{ij}^{(1)} \left( \frac{\alpha_s}{4\pi} \right)^2 + \mathcal{O}(\alpha_s^3), \quad (2.6.8)$$

where  $\gamma_{ij}^{(0)}$  do not commute with  $\gamma_{ij}^{(1)}$ . Therefore, in order to solve Eq. (2.6.6) we define an evolution operator such that

$$C_i(\mu) = U_{ij}(\mu, \mu_0) C_j(\mu_0), \quad (2.6.9)$$

and a leading order (LO) one can write

$$U^{(0)}(\mu, \mu_0) = \left[ \frac{\alpha(\mu)}{\alpha(\mu_0)} \right]^{-\frac{\gamma^{(0)T}}{2\beta_0}} = V \left( \left[ \frac{\alpha(\mu_0)}{\alpha(\mu)} \right]^{\frac{\gamma^{(0)}}{2\beta_0}} \right)_D V^{-1}, \quad (2.6.10)$$

where V diagonalizes the matrix  $\gamma^{(0)T}$  (matrix comprising of eigenvalues of  $\gamma^{(0)}$ ) such that

$\gamma_D^{(0)} = V^{-1}\gamma^{(0)T}V$ . To obtain the solution at the NLO

$$U(\mu, \mu_0) = \left[ 1 + \frac{\alpha_s(\mu)}{4\pi} J \right] U^{(0)}(\mu, \mu_0) \left[ 1 + \frac{\alpha_s(\mu_0)}{4\pi} J \right], \quad (2.6.11)$$

and if  $J = VHV^{-1}$  then Eq (2.6.11) promises the solution of Eq (2.6.7). The elements of matrix  $H$  can be written as

$$H_{ij} = \delta_{ij}\gamma_i^{(0)} \frac{\beta_1}{2\beta_0} - \frac{G_{ij}}{2\beta_0 + \gamma_i^{(0)} - \gamma_j^{(0)}}, \quad (2.6.12)$$

with the property that  $G = V^{-1}\gamma^{(1)T}V$ .

The WC's  $C_{7,8}^{eff}$  are generally used instead of  $C_{7,8}$  that include not only  $C_{7,8}$  but also the contribution of  $C_1 \cdots C_6$  and these can be expressed as

$$C_7^{eff} = C_7(\mu) + \sum_{i=1}^6 y_i C_i(\mu), \quad C_8^{eff} = C_8(\mu) + \sum_{i=1}^6 z_i C_i(\mu). \quad (2.6.13)$$

In the NDR scheme  $y = (0, 0, -1/3, -4/9, -20/3, -8/9)$  and  $z = (0, 0, 1, -1/6, 20, -10/3)$ . At the LO,  $C_{7,8}^{eff}$  depend on regularization scheme. The effective Hamiltonian in this case will be expressed in the following form

$$\mathcal{H}_{eff}(b \rightarrow s) = \frac{4G_F}{\sqrt{2}} \left( \lambda_{us} \sum_{i=1}^2 C_i \mathcal{O}_i^u + \lambda_{cs} \sum_{i=1}^2 C_i \mathcal{O}_i^c - \lambda_{ts} \sum_{i=8}^{10} C_i \mathcal{O}_i + h.c \right). \quad (2.6.14)$$

Here  $\lambda_{qs} = V_{qb}V_{qs}^*$  and the quark operators are define as,

$$\begin{aligned} \mathcal{O}_1 &= (\bar{s}_L \gamma_\mu T^a q_L) (\bar{q}_L \gamma^\mu T^a b_L), & \mathcal{O}_2 &= (\bar{s}_L \gamma_\mu q_L) (\bar{q}_L \gamma^\mu b_L), \\ \mathcal{O}_3 &= (\bar{s}_L \gamma_\mu b_L) \sum_q (\bar{q} \gamma^\mu q), & \mathcal{O}_4 &= (\bar{s}_L \gamma_\mu T^a b_L) \sum_q (\bar{q} \gamma^\mu T^a q), \end{aligned}$$

$$\begin{aligned}
\mathcal{O}_5 &= (\bar{s}_L \gamma_\mu \gamma_\nu \gamma_\alpha b_L) \sum_q (\bar{q} \gamma^\mu \gamma^\nu \gamma^\alpha q), & \mathcal{O}_6 &= (\bar{s}_L \gamma_\mu \gamma_\nu \gamma_\alpha T^a b_L) \sum_q (\bar{q} \gamma^\mu \gamma^\nu \gamma^\alpha T^a q), \\
\mathcal{O}_7 &= \frac{e}{16\pi^2} m_b (\bar{s}_L \sigma^{\mu\nu} b_R) F_{\mu\nu}, & \mathcal{O}_8 &= \frac{g_s}{16\pi^2} m_b (\bar{s}_L \sigma^{\mu\nu} T^a b_R) G_{\mu\nu}^a, \\
\mathcal{O}_9 &= \frac{e^2}{16\pi^2} (\bar{s}_L \gamma^\mu b_L) \sum_l (\bar{l} \gamma_\mu l), & \mathcal{O}_{10} &= \frac{e^2}{16\pi^2} (\bar{s}_L \gamma^\mu b_L) \sum_l (\bar{l} \gamma_\mu \gamma_5 l),
\end{aligned} \tag{2.6.15}$$

Here  $\mathcal{O}_1$  and  $\mathcal{O}_2$  are the current-current operators,  $\mathcal{O}_{3-6}$  are the QCD penguin operators,  $\mathcal{O}_7$  is the EM dipole operator,  $\mathcal{O}_8$  is a chromomagnetic dipole operator,  $\mathcal{O}_9$  and  $\mathcal{O}_{10}$  are semileptonic operators and the light quarks are denoted by  $q$ . The letter  $R$  and  $L$  means right and left-handed chiralities of the fermions. Some of the above operators get significant shares from renormalisation group mixing with  $\mathcal{O}_2$  generated at tree level and this decrease the NP effects. Hence it is considered sufficient to modify dipole and semileptonic operators in most of the NP scenarios. The chirality flipped counterparts of these SM operators are

$$\begin{aligned}
\mathcal{O}'_7 &= \frac{e}{16\pi^2} m_b (\bar{s}_R \sigma^{\mu\nu} b_L) F_{\mu\nu}, & \mathcal{O}'_8 &= \frac{g_s}{16\pi^2} m_b (\bar{s}_R \sigma^{\mu\nu} T^a b_L) G_{\mu\nu}^a, \\
\mathcal{O}'_9 &= \frac{e^2}{16\pi^2} (\bar{s}_R \gamma^\mu b_R) (\bar{l} \gamma_\mu l), & \mathcal{O}'_{10} &= \frac{e^2}{16\pi^2} (\bar{s}_R \gamma^\mu b_R) (\bar{l} \gamma_\mu \gamma_5 l).
\end{aligned} \tag{2.6.16}$$

The semileptonic unprimed and primed operators with different lepton flavors are

$$\mathcal{O}_9^{(l)} = \frac{e^2}{16\pi^2} (\bar{s}_{L,R} \gamma^\mu b_{L,R}) (\bar{l}_1 \gamma_\mu l_2), \quad \mathcal{O}_{10}^{(l)} = \frac{e^2}{16\pi^2} (\bar{s}_{L,R} \gamma^\mu b_{L,R}) (\bar{l}_1 \gamma_\mu \gamma_5 l_2). \tag{2.6.17}$$

The corresponding WC's of four-quark operators hold some symmetry relations such as Minimal flavor violation (MFV) of quarks give  $(C_i)_d = (C_i)_s$  and  $C'_i \approx 0$ . Lepton flavor violation (LFV) gives  $(C'_i)_q^e = (C'_i)_q^\mu = (C'_i)_q^\tau$  and lepton flavor conservation gives  $(C'_k)_q^{l_1 l_2}$ . The unitarity of CKM matrix leads to  $\lambda_{us} + \lambda_{cs} + \lambda_{ts} = 0$  which further implies that  $\lambda_{cs,ts} \sim \lambda^2 \gg \lambda_{us} \sim \lambda^4$ . Its consequence is that current-current operators  $\mathcal{O}_1^u$  and  $\mathcal{O}_2^u$  can be neglected and also  $\lambda_{ts} \sim -\lambda_{cs}$  can be predicted which leads to small CP asymmetries in the SM. Including electroweak corrections, the generalized effective Hamiltonian can be written as

$$\mathcal{H}_{eff} = \frac{G_F}{\sqrt{2}} \sum V_{CKM}^i C_i(\mu) \mathcal{O}_i(\mu), \tag{2.6.18}$$



where  $V_{CKM}^i$  are the elements of CKM matrix. Decay amplitude for Hadron  $H$  is

$$\mathcal{A}(H_i \rightarrow X) = \langle X | \mathcal{H}_{eff} | H_i \rangle = \frac{G_F}{\sqrt{2}} \sum V_{CKM}^i C_i(\mu) \langle X | \mathcal{O}_i(\mu) | H_i \rangle, \quad (2.6.19)$$

where  $X$  is the possible final state and  $C_i(\mu)$  and  $\mathcal{O}_i(\mu)$  are the functions of  $M_W$ , coupling constant  $\alpha_s$  and renormalization scale  $\mu$ . One can get the WC's by matching the results of full theory with an effective theory.

## 2.7 Hadrons

The bottom quark belong to the third generation of quarks and is a weak doublet partner of top quark. Kobayashi and Maskawa in 1973 [26] introduced bottom and top quarks, which experimentally confirmed in 1977 by the production of  $b\bar{b}$  state. Meson containing light quark (i.e.  $u, d, s, c$ ) with  $b$ -quark are called  $B^+, B^0, B_s^0$  and  $B_c^+$ , respectively.  $B_c^+$  contain both  $b$  and  $c$ -quark is the heaviest one in all of the bound states and its difficult to produce. It was first produced in 1998 by CDF collaborator [27] and from the decay  $B_c^+ \rightarrow J/\psi\pi^+$  its mass was determined by the CDF collaboration in 2006 [28]. However, the LHCb published its most accurate mass of  $m_{B_c^+} = 6274.28 \pm 1.40 \pm 0.32 MeV/c^2$  through the decay  $B_c^+ \rightarrow J/\psi D^0 K^+$  [29]. The  $\Lambda_b$  baryon is one of the  $b$ -quark bound state containing  $u, d, b$  quarks has its prime importance.

The FCNC decays governed by  $b \rightarrow sl^+l^-$  are studied as a function of dilepton mass squared  $s \equiv q^2$ . In the measurements, the regions  $J/\psi$  and  $\psi(2s)$  are usually not included due to dominance of  $b \rightarrow c$  transitions. Hence, the most reliable measurements are at low and high  $s$  regions and in these regions one can compare the experimental measurements with the theoretical predictions.

High energy  $pp$  collision at the LHC and  $p\bar{p}$  collision at the Tevatron produce all kinds of  $b$ -hadrons. Tevatron produces cross-section of  $30\mu b$  for  $(p\bar{p} \rightarrow bX)$  with pseudorapidity  $\eta < 1$  at  $\sqrt{s} = 1.96$  TeV where as LHCb produces about  $72\mu b$  at 7 TeV and about  $144\mu b$  at 13 TeV with pseudorapidity  $2 < \eta < 5$ . Among the weak decays of  $b$ -hadrons, the dominant decay process is  $b \rightarrow cW^{*+}$  as  $b \rightarrow c$  decay is suppressed by the factor of  $|V_{ub}|/|V_{uss}| \sim (0.1)^2$  as compared

to the decay  $b \rightarrow c$ . Due to color suppression, the decay modes in which the spectator quark combines with the virtual W boson to form bound hadronic state are suppressed by a factor of  $(1/3)^2$  because color of both quarks has to be the same. Decay mode  $B \rightarrow X_c l \nu$  for  $V_{ub}$  as final state with two leptons make the study of strong interactions to be much easier. Both inclusive and exclusive analysis can be used for this purpose but both are accompanied by uncertainties. Inclusive analysis include uncertainties that belong to extrapolation of restricted phase-space to full phase where as exclusive decays have uncertainties belonging to hadronic Form Factors. For inclusive analysis, differential decays rates of all the  $B$ -meson decays governed by the transition  $b \rightarrow ul\nu$  give  $|V_{ub}| = (4.41 \pm 0.15_{-0.17}^{+0.15}) \times 10^{-3}$ , where the uncertainties correspond to both the experimental measurements and the theoretical calculations [30]. The analysis of exclusive decays is comparatively simple from experimental point of view in which the branching ratio of a particular decay is used to calculate the CKM matrix element under consideration by using Form Factors calculated in LQCD or QCD sum rules (QCDSR) approach. The world average of this analysis gives  $|V_{ub}| = (3.28 \pm 0.29) \times 10^{-3}$ , which is the average obtained from the semileptonic  $B$  decays, An expected result was obtained in 2015 when LHCb measured CKM matrix element  $V_{ub}$  by the ratio [31]

$$\frac{|V_{ub}|^2}{|V_{cb}|^2} = \frac{\mathcal{B}_r(\Lambda_b^0 \rightarrow p\mu^-\bar{\nu}_\mu)}{\mathcal{B}_r(\Lambda_b^0 \rightarrow \Lambda_c^+\mu^-\bar{\nu}_\mu)} R_{FF}, \quad (2.7.1)$$

where  $R_{FF}$  is the ratio of relevant Form Factors calculated using LQCD approach. Using  $R_{FF} = 0.68 \pm 0.07$  the above ratio comes out to be  $0.083 \pm 0.004 \pm 0.004$  where the experimental uncertainty first and the second one belongs to LQCD prediction. The world average for  $|V_{cb}| = (39.5 \pm 0.8) \times 10^{-3}$ ,  $|V_{ub}| = (3.27 \pm 0.15 \pm 0.16 \pm 0.06) \times 10^{-3}$  where third uncertainty belongs to  $V_{cb}$  normalization.

According to world average presented in [31]

$$V_{cs} = 0.9746 \pm 0.0026, \quad V_{cd} = 0.2140 \pm 0.0097, \quad (2.7.2)$$

which are compatible with unitary of CKM matrix.

## 2.8 Flavor Physics

Within the Standard Model (SM), fermions are organized into three distinct generations, and flavor physics involves the study of interactions that differentiate between these generations. Fermions can interact through two main mechanisms: Yukawa couplings, where two fermions couple with a scalar, and gauge interactions, where fermions couple through gauge bosons. Interactions between different generations of fermions lack gauge couplings in the interaction eigenstate, and each type of gauge coupling is defined by a single coupling constant. Consequently, gauge interactions are diagonal and universal when considered in the interaction basis. On the other hand, Yukawa couplings involve interactions between different fermion generations, and their interaction eigenstates do not possess definite masses. However, once transformed into the mass eigenstate basis, Yukawa interactions become diagonal but non-universal, and the fermions acquire definite masses.

Flavor physics holds unique significance in both the quark and lepton sectors, as it offers significant potential for predicting New Physics (NP) indirectly, even before direct experimental observations. The success of past flavor physics predictions is evident, such as the prediction of the charm quark through the small ratio of decay widths of  $K_L \rightarrow \mu_+\mu_-$  to  $K^+ \rightarrow \mu_+\nu$  the anticipation of the third generation via neutral kaon mixing involving CP violation, the determination of the masses of charm and top quarks, and the observation of flavor transitions in neutrinos that implies the existence of massive neutrinos.

The investigation of rare processes like  $B_S \rightarrow \mu^+\mu^-$  has been conducted extensively and their measurements are well established. In the SM, these rare processes are forbidden at the tree level and only arise through loop diagrams via mechanisms like the Glashow-Iliopoulos-Maiani (GIM) mechanism [32]. These rare processes are further suppressed by the small off-diagonal entries in the Cabibbo-Kobayashi-Maskawa (CKM) matrix. Additionally, decays involving leptons in the final states, such as muons and electrons, are subject to helicity suppression due to the emission of two spin-1/2 leptons from a pseudoscalar B-meson. Several predictions for B decays within the SM are available, offering insights into various rare decay

modes.

$$\begin{aligned}
\mathcal{B}(\bar{B}_s \rightarrow l^+l^-) &= (8.34 \pm 0.36) \times 10^{-14}, & \mathcal{B}(B^0 \rightarrow l^+l^-) &= (2.63 \pm 0.32) \times 10^{-15}, \\
\mathcal{B}(\bar{B}_s \rightarrow \mu^+\mu^-) &= (3.52 \pm 0.15) \times 10^{-9}, & \mathcal{B}(B^0 \rightarrow \mu^+\mu^-) &= (1.12 \pm 0.12) \times 10^{-10}, \\
\mathcal{B}(\bar{B}_s \rightarrow \tau^+\tau^-) &= (7.46 \pm 0.30) \times 10^{-7}, & \mathcal{B}(B^0 \rightarrow \tau^+\tau^-) &= (2.35 \pm 0.24) \times 10^{-8}.
\end{aligned} \tag{2.8.1}$$

During the Run 1 of LHC, the combined results of CMS and LHCb datasets performed in 2014 comes out to be [33]

$$\begin{aligned}
\bar{\mathcal{B}}(B_s \rightarrow \mu^+\mu^-) &= (2.8_{-0.6}^{+0.7}) \times 10^{-9}, \\
\mathcal{B}(B^0 \rightarrow \mu^+\mu^-) &= (3.9_{-1.4}^{+1.6}) \times 10^{-10}.
\end{aligned} \tag{2.8.2}$$

Since weak and Higgs mediated processes are strongly suppressed in the SM, the FCNCs can take place at higher levels only in electroweak interactions, thus they are good candidates to search for the NP.

The CELLO experiments in 1994 studied the rare radiative decays process  $b \rightarrow s\gamma$  [34]. Later in 2008 and 2010, BaBar and Belle collected a dataset of 467M and 772M  $B^0\bar{B}^0$  pairs and their combined dataset produced an integrated luminosity of  $1ab^{-1}$  operating at  $\Gamma(4S)$ . At LHC,  $b\bar{b}$  cross-section is about  $300\mu b$  at center of mass energy  $\sqrt{s} = 7$  TeV [35] and  $500\mu b$  at  $\sqrt{s} = 14$  TeV, providing  $10^{11}$  hadrons produced in a dataset of  $1fb^{-1}$ . At LHC, the experiments contributing to rare  $b$ -hadron decays are the LHCb, CMS and the ATLAS. The CMS and ATLAS experiments are able to produce dimuon pair in the final states, whereas LHCb can generate photon, dilepton pair and only hadrons as final states. In semileptonic decays, initially B factories used to average over neutral and charged  $B$ -mesons and also between  $\bar{\mu}\mu$  and  $\bar{l}l$  final states. The LHCb, CMS, ATLAS and CDF experiments measure the decays with  $\mu^+\mu^-$  and  $l^+l^-$  final states mostly instead of  $l^+l^-$  final states. In last two decades, the processes  $B \rightarrow K^*(892)^0l^+l^-$  and  $B \rightarrow K^+l^+l^-$  have been widely studied. The CDF and LHCb also observed other  $b$ -hadron decays such as  $\Lambda_b^0 \rightarrow \Lambda\mu^+\mu^-$  [36],  $\Lambda_b^0 \rightarrow pK\mu^+\mu^-$  [37] and  $B_s^0 \rightarrow \phi\mu^+\mu^-$  [38]. The measured branching fractions of some commonly studied  $b$ -hadron decays are

$$\mathcal{B}(B^+ \rightarrow K^+l^+l^-) = (5.5 \pm 0.7) \times 10^{-7},$$

$$\begin{aligned}
\mathcal{B}(B^+ \rightarrow K^+ \mu^+ \mu^-) &= (4.43 \pm 0.24) \times 10^{-7}, \\
\mathcal{B}(B^0 \rightarrow K^*(892)^0 l^+ l^-) &= (1.03_{-0.17}^{+0.19}) \times 10^{-6}, \\
\mathcal{B}(B^0 \rightarrow K^*(892)^0 \mu^+ \mu^-) &= (1.03 \pm 0.06) \times 10^{-6}, \\
\mathcal{B}(B_s^0 \rightarrow \phi \mu^+ \mu^-) &= (8.3 \pm 1.2) \times 10^{-7}, \\
\mathcal{B}(\Lambda_b^0 \rightarrow \Lambda \mu^+ \mu^-) &= (1.08 \pm 0.28) \times 10^{-6}, \tag{2.8.3}
\end{aligned}$$

Compared to the leptonic and radiative decays of  $B$ -meson the semileptonic one are quite rich in the phenomenology. The next chapters discuss the rare  $\Lambda_b \rightarrow \Lambda \gamma$  and  $\Lambda_b \rightarrow \Lambda \mu^+ \mu^-$  decays in the SM.

# Chapter 3

## Helicity Formalism of decay

### $\Lambda_b^0 \rightarrow \Lambda^0 Z_c^0 (3900)$ in SM

#### 3.1 Introduction

The  $\Lambda_b$  baryon, which consists of a bottom quark and two light quarks (up and down), serves as an isospin singlet ground state within the  $b$ -baryon family. Studying its decays provides valuable insights into the underlying physics of QCD and contributes to model development. Similar to  $B$ -mesons, the decays of  $\Lambda_b$  allow for measurements of various properties, including masses, lifetimes, and branching fractions. In 2011, the CDF collaboration made the initial measurement of the  $\Lambda_b$  baryon decay  $\Lambda_b \rightarrow \Lambda \mu^+ \mu^-$  [39]. The Tevatron experiments determined the characteristic properties (mass and lifetime) of the  $\Lambda_b$  baryon through two decay modes:  $\Lambda_b \rightarrow \Lambda J/\psi$  and  $\Lambda_b \rightarrow \Lambda_c^+ \pi^-$  [40]. Since December 2009, the LHCb experiment has been dedicated to studying the production of  $b$ -hadrons, with a production ratio of  $B^0 : \Lambda_b^0 : B_c^0 = 4 : 2 : 1$ . The high rate of  $b$ -hadron production at LHCb allows for the observation of Cabibbo-suppressed decay modes of  $\Lambda_b$  baryons, such as  $\Lambda_b \rightarrow D p K^-$ ,  $\Lambda_b \rightarrow \Lambda_c^+ K^-$  [41],  $\Lambda_b \rightarrow \Lambda_c^+ D^-$ ,  $\Lambda_b \rightarrow \Lambda_c^+ D_s^-$  [41], and  $\Lambda_b \rightarrow J/\psi p \pi^-$  [42]. LHCb has also measured multi-body decays of  $\Lambda_b$ , including  $\Lambda_b \rightarrow \Lambda K^+ \pi^-$ ,  $\Lambda_b \rightarrow \Lambda K^+ K^-$ ,  $\Lambda_b \rightarrow p K^- \pi^+ \pi^-$ ,  $\Lambda_b \rightarrow p K^- K^+ K^-$ ,  $\Lambda_b \rightarrow \psi(2S) p K^-$ , and  $\Lambda_b \rightarrow J/\psi \pi^+ \pi^- p K^-$  [43]. LHCb achieved the most precise measurement of the  $\Lambda_b$  mass, obtaining a value of  $5620 \pm 0.31$  (stats)  $\pm 0.47$  (sys).

BESIII Collaboration in 2013 analyzed the process  $e^+ e^- \rightarrow \pi^+ \pi^- J/\psi$  at  $\sqrt{s} = 4.26$  GeV

[44]. With the analysis of invariant mass spectrum of  $\pi^\pm J/\psi$  suggest that there exist interesting substructure as which latter known as  $Z_c^\pm$  (3900) and its confirmation came by Belle and CLEO-c experiments [45, 46] along with its neutral partner  $Z_c^0$  (3900). This chapter is dedicated to study the helicity formalism of the semileptonic four body  $\Lambda_b^0 \rightarrow \Lambda^0 Z_c^0$  (3900) decay.

### 3.1.1 Generation of Tetraquark States via Weak Decays of B-Baryons

Here, we commence by constructing the representations for hadron multiplets using the framework of the flavor  $SU(3)$  group. Our specific focus lies on b-baryons, which are categorized into antitriplet and sextet multiplets denoted as  $\mathcal{B}$  and  $\mathcal{C}$ , respectively. Comprising three light quarks, light baryons exhibit the following structure:

$$T_8 = \begin{pmatrix} \frac{1}{\sqrt{2}}\Sigma^0 + \frac{1}{\sqrt{6}}\Lambda^0 & \Sigma^+ & p \\ \Sigma^- & -\frac{1}{\sqrt{2}}\Sigma^0 + \frac{1}{\sqrt{6}}\Lambda^0 & n \\ \Xi^- & \Xi^0 & -\sqrt{\frac{2}{3}}\Lambda^0 \end{pmatrix}, \quad (3.1.1)$$

which can be derived as Baryon has baryon number  $B = 1$  and they are made up of three quarks so

$$\begin{aligned} q_j q_k &= \frac{1}{2} (q_j q_k + q_k q_j) + \frac{1}{2} (q_j q_k - q_k q_j) \\ &= \frac{1}{\sqrt{2}} S_{jk} + \frac{1}{\sqrt{2}} A_{jk}. \end{aligned} \quad (3.1.2)$$

Here the symmetric tensor has six independent components

$$S_{jk} = \frac{1}{\sqrt{2}} (q_j q_k + q_k q_j).$$

Similarly, the anti-symmetric tensor is written as following, having three independent components.

$$A_{jk} = \frac{1}{\sqrt{2}} (q_j q_k - q_k q_j),$$

where  $i, j$  denotes the indices and  $q_j$  and  $q_k$  are the field operators. Let's define

$$q_j = \begin{pmatrix} q_1 \\ q_2 \\ q_3 \end{pmatrix} = \begin{pmatrix} \bar{u} \\ \bar{d} \\ \bar{c} \end{pmatrix}$$

as the field operator which creates a  $u$ -quark, a  $d$ -quark or a  $s$ -quark

$$\bar{u}|0\rangle = |u\rangle, \bar{d}|0\rangle = |d\rangle, \bar{s}|0\rangle = |s\rangle.$$

The field operator belong to the representation  $\bar{3}$  of  $SU(3)$ , whereas the field operator

$$q^j = \begin{pmatrix} q^1 \\ q^2 \\ q^3 \end{pmatrix} = \begin{pmatrix} u \\ d \\ s \end{pmatrix}$$

pertains to the  $\bar{3}$  representation in the context of  $SU(3)$ , distinct from the 3 representation due to its transformation behavior. Specifically, the matrix notation employs  $q_j$  and  $q^j$  to denote the field operator as a column matrix and row matrix respectively. It's important to note that  $q^j$  either creates an anti-quark or annihilates quarks, while the  $\bar{3}$  representation's unique attribute is rooted in the distinction between quarks and anti-quarks. This differentiation is characterized by the hypercharge, and it is imperative to recognize that the  $\bar{3}$  representation's transformation property is such that  $q^j = q_j$ .

$$\bar{q} = \begin{pmatrix} \bar{u} & \bar{d} & \bar{s} \end{pmatrix}$$

$$q = \begin{pmatrix} u \\ d \\ s \end{pmatrix}$$



Now a vector  $F^i$  belonging to the representation  $\bar{3}$  can be written as

$$\begin{aligned} F^i &= \epsilon^{ilm} A_{lm} \\ A_{jk} &= \frac{1}{2} \epsilon_{ijk} F^i. \end{aligned} \quad (3.1.3)$$

We have the results

$$3 \otimes 3 \otimes 3 = (6 \otimes 3) \oplus (\bar{3} \otimes 3).$$

First consider  $\bar{3} \otimes 3$

$$F^i q_j = \left( F^i q_j - \frac{1}{3} \delta_j^i T^k q_k \right) + \frac{1}{3} \delta_j^i F^k q_k \quad (3.1.4)$$

$\bar{3} \otimes 3 = 8 \oplus 1$ . The octet operator for the baryons can be written as

$$\bar{T}_j^i = \frac{1}{2} \left( F^i q_j - \frac{1}{3} \delta_j^i T^k q_k \right), \quad (3.1.5)$$

where

$$F^i = \epsilon^{ilm} A_{lm} = \frac{1}{2\sqrt{6}} \epsilon^{ilm} (q_l q_m - q_m q_l). \quad (3.1.6)$$

Now lets consider  $6 \otimes 3$ . It is given by

$$\begin{aligned} S_{ij} q_{kl} &= S_{ij} q_k + S_{jk} q_i + S_{ki} q_j - S_{jk} q_i - S_{ki} q_j \\ &= \tilde{F}_{\{i,j,k\}} - S_{jk} q_i - S_{ki} q_j, \end{aligned} \quad (3.1.7)$$

with

$$\tilde{F}_{\{i,j,k\}} = S_{ij} q_k + S_{jk} q_i + S_{ki} q_j \quad (3.1.8)$$

is completely symmetric tensor and has 10 independent components. So we have  $6 \otimes 3 = 10 \oplus 8$

. We write the decouplet representation

$$\begin{aligned} \tilde{F}_{\{i,j,k\}} &= \sqrt{3} \tilde{F}_{\{i,j,k\}} \\ &= \frac{1}{\sqrt{3}} [S_{ij} q_k + S_{jk} q_i + S_{ki} q_j] \end{aligned} \quad (3.1.9)$$

and the octet representation

$$\tilde{T}_\gamma^l = \frac{1}{\sqrt{3}} \epsilon^{lmn} S_{\gamma n} q_m \quad (3.1.10)$$

$$\tilde{T}_l^l = 0$$

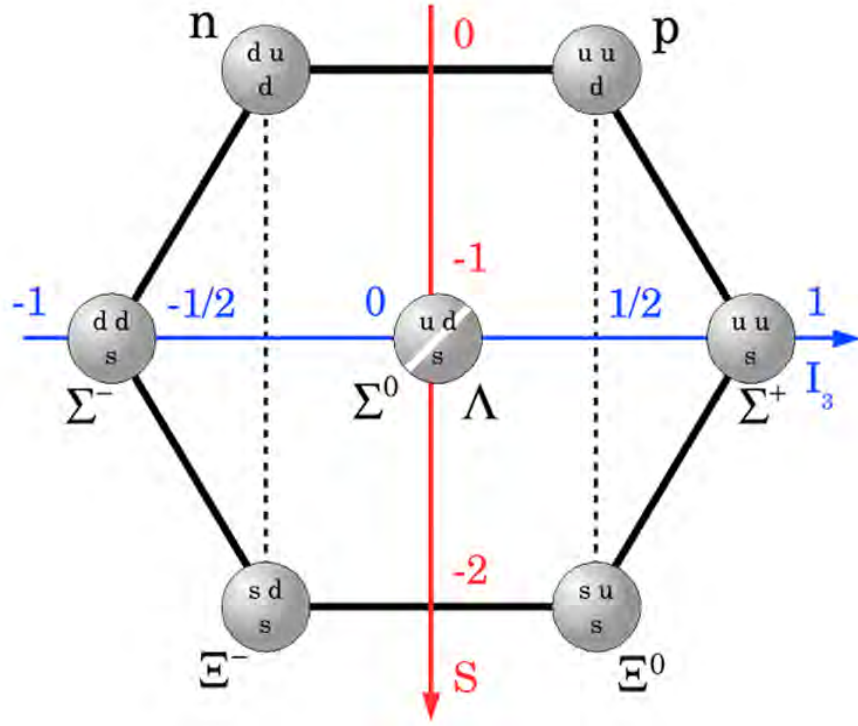
so the final representation has the form

$$\begin{aligned} 3 \otimes 3 \otimes 3 &= (6 \otimes \bar{3}) \otimes 3 = (6 \otimes 3) \oplus (\bar{3} \otimes 3) \\ &= 10 \oplus 8 \oplus 8' \oplus 1. \end{aligned} \quad (3.1.11)$$

This gives

$$\begin{aligned} \bar{T}_j^i |0\rangle &= |T_j^i\rangle \\ &= \frac{1}{2\sqrt{2}} \left[ \epsilon^{ilm} (q_l q_m - q_m q_l) q_j - \frac{1}{3} \delta_j^i \epsilon^{klm} (q_l q_m - q_m q_l) q_k \right] |0\rangle. \end{aligned} \quad (3.1.12)$$

By considering state 8,  $|p\rangle = \bar{B}_1^3 |0\rangle$ , the quark content is  $\frac{1}{\sqrt{2}} | [u, d] u \rangle$ . Similarly the quark content of  $|n\rangle = \bar{B}_2^3 |0\rangle$  is  $\frac{1}{\sqrt{2}} | [u, d] d \rangle$ . The quark content of  $|\Sigma^+\rangle = \bar{B}_1^2 |0\rangle$  is  $\frac{1}{\sqrt{2}} | [u, s] u \rangle$ . The quark content of  $|\Sigma^0\rangle = \frac{1}{\sqrt{2}} (\bar{B}_1^1 |0\rangle - \bar{B}_2^2 |0\rangle)$  is  $\frac{1}{\sqrt{2}} | [s, d] u + [u, s] d \rangle$ . The quark content of  $|\Sigma^-\rangle = \bar{B}_2^1 |0\rangle$  is  $\frac{1}{\sqrt{2}} | [d, s] d \rangle$ . The quark content of  $|\Lambda^0\rangle = \frac{-3}{\sqrt{6}} \bar{B}_3^3 |0\rangle$  is  $\frac{1}{\sqrt{2}} | 2 [u, d] s \rangle - [d, s] u - [s, u] d$ . Similarly the quark content of  $|\Xi^-\rangle = \bar{B}_3^1 |0\rangle$  is  $\frac{1}{\sqrt{2}} | [d, s] s \rangle$  and of the  $\Xi^0$  is  $\frac{1}{\sqrt{2}} | [s, u] s \rangle$ .


 Figure 3.1.1: Octet representing arrangement of  $n, p, \Sigma^-, \Sigma^0, \Sigma^+, \Xi^-, \Xi^0, \Lambda^0$  [55]

Similarly the state  $8'$  has the quark content as following:

$$\begin{aligned}
 \bar{B}_1^3 |0\rangle &: \frac{1}{\sqrt{6}} |([u, d]_+ u - 2uud)\rangle \\
 \bar{B}_1^2 |0\rangle &: \frac{1}{\sqrt{6}} |([u, s]_+ u - 2uus)\rangle \\
 \frac{1}{\sqrt{2}} (\bar{B}_1^1 - \bar{B}_2^2) |0\rangle &: \frac{1}{\sqrt{12}} |(-2[u, d]_+ s + [u, s]_+ d + [d, s]_+ u)\rangle \\
 \bar{B}_1^2 &: \frac{1}{\sqrt{6}} |([d, s]_+ d - 2dds)\rangle \\
 \frac{-3}{\sqrt{6}} \bar{B}_3^3 |0\rangle &: \frac{-1}{2} |([s, d]_+ u - [s, u]_+ d)\rangle \\
 \bar{B}_3^1 |0\rangle &: \frac{1}{\sqrt{6}} |(2ssd - [d, s]_+ s)\rangle \\
 \bar{B}_3^2 |0\rangle &: \frac{1}{\sqrt{6}} |([s, u]_+ s - 2ssu)\rangle
 \end{aligned}$$

For the representation of  $8'$ , we can define

$$\bar{T}_j^i |0\rangle = |T_j^i\rangle = \frac{1}{2\sqrt{3}} \epsilon^{ikl} S_{jl} q_k |0\rangle \quad (3.1.13)$$

So we see that  $3 \times 3$  matrices can be represented as

$$T_8 = T_j^i = \begin{pmatrix} \frac{1}{\sqrt{2}}\Sigma^0 + \frac{1}{\sqrt{6}}\Lambda^0 & \Sigma^+ & p \\ \Sigma^- & -\frac{1}{\sqrt{2}}\Sigma^0 + \frac{1}{\sqrt{6}}\Lambda^0 & n \\ \Xi^- & \Xi^0 & -\sqrt{\frac{2}{3}}\Lambda^0 \end{pmatrix}$$

$$\bar{T}_j^i = \begin{pmatrix} \frac{1}{\sqrt{2}}\bar{\Sigma}^0 + \frac{1}{\sqrt{6}}\Lambda^0 & \bar{\Sigma}^+ & \bar{p} \\ \bar{\Sigma}^- & -\frac{1}{\sqrt{2}}\bar{\Sigma}^0 + \frac{1}{\sqrt{6}}\bar{\Lambda}^0 & \bar{n} \\ \bar{\Xi}^- & \bar{\Xi}^0 & -\sqrt{\frac{2}{3}}\bar{\Lambda}^0 \end{pmatrix}. \quad (3.1.14)$$

Note that

$$\bar{T}_j^i = \gamma^0 T_j^{*i}.$$

Note that, the matrix notation for row is represented by  $(i)$  and for column is represented by  $(j)$ , with complex conjugation  $(*)$ , in the context of  $SU(3)$  and field operators. Similarly we can also calculate the  $\mathcal{B}_{ij}$  and  $\mathcal{C}_{ij}$  as

$$\mathcal{B}_{ij} = \begin{pmatrix} 0 & \Lambda_b^0 & \Xi_b^0 \\ -\Lambda_b^0 & 0 & \Xi_b^- \\ -\Xi_b^0 & -\Xi_b^- & 0 \end{pmatrix}, \quad (3.1.15)$$

$$\mathcal{C}_{ij} = \begin{pmatrix} \Sigma_b^+ & \frac{\Sigma_b^0}{\sqrt{2}} & \frac{\Xi_b'^0}{\sqrt{2}} \\ \frac{\Sigma_b^0}{\sqrt{2}} & \Sigma_b^- & \frac{\Xi_b^-}{\sqrt{2}} \\ \frac{\Xi_b'^0}{\sqrt{2}} & \frac{\Xi_b^-}{\sqrt{2}} & \Omega \end{pmatrix}. \quad (3.1.16)$$

In the same way, components of tetraoctet are

$$(\mathcal{Z}_c)_{ij} = \begin{pmatrix} \frac{Z_{c\pi^0}}{\sqrt{2}} + \frac{Z_{c\eta_8}}{\sqrt{6}} & Z_{c\pi^+} & Z_{cK^+} \\ Z_{c\pi^-} & -\frac{Z_{c\pi^0}}{\sqrt{2}} + \frac{Z_{c\eta_8}}{\sqrt{6}} & Z_{cK^0} \\ Z_{cK^-} & Z_{c\bar{K}^0} & -2\frac{Z_{c\eta_8}}{\sqrt{6}} \end{pmatrix}. \quad (3.1.17)$$

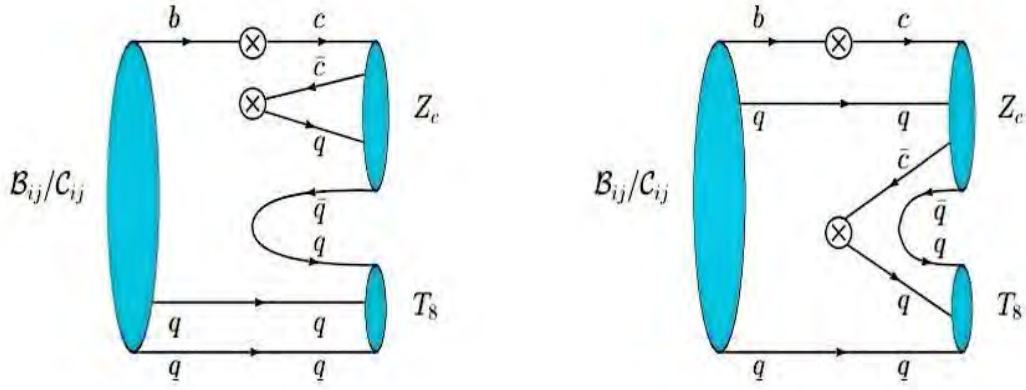


Figure 3.1.2: Feynman Diagram Depicting the Octet Tetraquark and Light Baryon Formation from the Decay of a b-Baryon[56]

The Hamiltonian governing the weak decay process of  $b$ -baryons into an octet tetraquark and a light baryon may be mathematically represented as follows:

$$\mathcal{H}_{eff}(b \rightarrow qc\bar{c}) = \frac{G_F}{\sqrt{2}} (V_{cb}V_{cq}^* (C_1O_1 + C_2O_2)), \quad (3.1.18)$$

with

$$O_1 = (\bar{c}_\alpha b_\beta)_{V-A} (\bar{q}_\beta c_\alpha)_{V-A}, O_2 = (\bar{c}_\alpha b_\alpha)_{V-A} (\bar{q}_\beta c_\beta)_{V-A},$$

where  $q$  denotes  $d$  or  $s$ .  $G_F$  stands for the Fermi coupling constant and  $V_{ij}$  denotes the CKM matrix element.  $O_i$  is the low energy operator and  $C_i$  denotes the Wilson coefficients.

When considering a b-baryon from the anti-triplet multiplet, its decay entails the transformation into an octet tetraquark and a light baryon, the effective Hamiltonian can be written as

$$\begin{aligned} \mathcal{H}_{eff} = & a_1(\mathcal{B})^{ij}(\mathcal{H}_3)_{ij}(\mathcal{Z}_c)_k^l(T^8)_l^k + a_2(\mathcal{B})^{ij}(\mathcal{H}_3)_{ik}(\mathcal{Z}_c)_k^l(T^8)_j^l + a_3(\mathcal{B})^{ij}(\mathcal{H}_3)_{il}(\mathcal{Z}_c)_j^k(T^8)_k^l + \\ & a_4(\mathcal{B})^{ij}(\mathcal{H}_3)_{kl}(\mathcal{Z}_c)_i^k(T^8)_j^l, \end{aligned} \quad (3.1.19)$$

In the case of a b-baryon existing within the sextet multiplet, the effective Hamiltonian is

expressed as follows:

$$\mathcal{H}_{eff} = b_1(\mathcal{C})^{ij}(\mathcal{H}_3)_{ik}(\mathcal{Z}_c)_k^l(T^8)_j^l + b_2(\mathcal{C})^{ij}(\mathcal{H}_3)_{il}(\mathcal{Z}_c)_j^k(T^8)_k^l + b_3(\mathcal{C})^{ij}(\mathcal{H}_3)_{kl}(\mathcal{Z}_c)_i^k(T^8)_j^l, \quad (3.1.20)$$

where  $a_i$  and  $b_i$  stands for the amplitudes. Numerous characteristics related to the weak decay processes of b-baryons into a tetraquark and a light baryon can be inferred from these outcomes. By performing sum over Hamiltonian and then expanding it, we get the amplitudes

$$\mathcal{A} = \sum_{ijk} \mathcal{H}_{eff},$$

where  $i, j, k$  is from 1 to 3. Exercising all the indices, we can write different amplitudes as:

$$\begin{aligned} A(\Lambda_b^0 \rightarrow Z_{c\pi^+}\Sigma^-) &= (2a_1 + a_2 + a_3 - a_4) \times V_{cs}^* \\ A(\Lambda_b^0 \rightarrow Z_{cK^-}p) &= (2a_1 + a_2) \times V_{cs}^* \\ A(\Lambda_b^0 \rightarrow Z_{c\pi^0}\Sigma^0) &= (2a_1 + a_2 + a_3 - a_4) \times V_{cs}^* \\ A(\Lambda_b^0 \rightarrow Z_{c\bar{K}^0}n) &= (2a_1 + a_2) \times V_{cs}^* \\ A(\Lambda_b^0 \rightarrow Z_{c\eta_8}\Lambda^0) &= \frac{1}{3}(6a_1 + a_2 + a_3 + a_4) \times V_{cs}^* \end{aligned}$$

$$\begin{aligned} A(\Xi_b^0 \rightarrow Z_{cK^-}\Sigma^+) &= (a_3 - a_4) \times V_{cs}^* \\ A(\Xi_b^0 \rightarrow Z_{c\bar{K}^0}\Sigma^0) &= \frac{1}{\sqrt{2}}(-a_3 + a_4) \times V_{cs}^* \\ A(\Xi_b^0 \rightarrow Z_{c\bar{K}^0}\Lambda^0) &= \frac{(-2a_2 + a_3 + a_4)}{\sqrt{6}} \times V_{cs}^* \\ A(\Xi_b^0 \rightarrow Z_{cK^-}\Sigma^0) &= \frac{1}{\sqrt{2}}(-a_3 + a_4) \times V_{cs}^* \\ A(\Xi_b^0 \rightarrow Z_{cK^-}\Lambda^0) &= \frac{(-2a_2 + a_3 + a_4)}{\sqrt{6}} \times V_{cs}^* \\ A(\Xi_b^0 \rightarrow Z_{c\bar{K}^0}\Sigma^-) &= (-a_3 + a_4) \times V_{cs}^* \end{aligned} \quad (3.1.21)$$

For  $c \rightarrow d$ , we have following amplitudes corresponding to each channel as

$$\begin{aligned}
A(\Lambda_b^0 \rightarrow Z_{c\pi^0} n) &= \frac{(a_3 - a_4)}{\sqrt{2}} V_{cd}^* \\
A(\Lambda_b^0 \rightarrow Z_{c\pi^-} p) &= (a_3 - a_4) V_{cd}^* \\
\\
A(\Lambda_b^0 \rightarrow Z_{cK^+} \Sigma^-) &= (a_4 - a_2) V_{cd}^* \\
A(\Lambda_b^0 \rightarrow Z_{cK^0} \Sigma^0) &= \frac{1}{\sqrt{2}} (a_4 - a_2) V_{cd}^* \\
A(\Lambda_b^0 \rightarrow Z_{cK^0} \Lambda^0) &= \frac{1}{\sqrt{6}} (-a_4 + a_2 - 2a_3) V_{cd}^* \\
A(\Lambda_b^0 \rightarrow Z_{c\eta_8} n) &= \frac{1}{\sqrt{6}} (-a_4 + 2a_2 - a_3) V_{cd}^* \\
A(\Xi_b^0 \rightarrow Z_{c\pi^0} \Lambda^0) &= \frac{1}{2\sqrt{3}} (-2a_4 + a_2 + a_3) V_{cd}^* \\
A(\Xi_b^0 \rightarrow Z_{c\pi^-} \Sigma^+) &= -(2a_1 + a_2) V_{cd}^* \\
A(\Xi_b^0 \rightarrow Z_{c\pi^0} \Sigma^0) &= -\frac{1}{2} (4a_1 + a_2 + a_3) \times V_{cd}^* \\
A(\Xi_b^0 \rightarrow Z_{c\bar{K}^0} n) &= -(2a_1 + a_3) V_{cd}^* \\
A(\Xi_b^0 \rightarrow Z_{c\eta_8} \Sigma^0) &= -\frac{(a_2 + a_3 - 2a_4)}{2\sqrt{3}} \times V_{cd}^* \\
A(\Xi_b^0 \rightarrow Z_{cK^-} p) &= -(2a_1 + a_2 + a_3) \times V_{cd}^* \\
A(\Xi_b^0 \rightarrow Z_{cK^-} n) &= (a_4 - a_2) \times V_{cd}^* \\
A(\Xi_b^0 \rightarrow Z_{c\eta_8} \Sigma^-) &= -\frac{(a_2 + a_3 - 2a_4)}{\sqrt{6}} \times V_{cd}^* \\
\\
A(\Xi_b^0 \rightarrow Z_{c\pi^0} \Sigma^-) &= \frac{(a_3 - a_2)}{\sqrt{2}} \times V_{cd}^* \\
A(\Xi_b^0 \rightarrow Z_{c\pi^-} \Lambda^0) &= \frac{-(a_2 + a_3 - 2a_4)}{\sqrt{6}} \times V_{cd}^* \\
A(\Xi_b^0 \rightarrow Z_{c\pi^0} \Sigma^0) &= \frac{(-a_3 + a_2)}{\sqrt{2}} \times V_{cd}^* \tag{3.1.22}
\end{aligned}$$

The  $c \rightarrow s$  transition is roughly proportional to  $|V_{cs}|$ , which is approximately 1, while the  $c \rightarrow d$  transition involves a CKM matrix element  $|V_{cd}|$ , which is approximately 0.2.

$$\begin{aligned}
A(\Sigma_b^+ \rightarrow Z_{c\pi^+} \Lambda^0) &= \frac{(b_1 + b_2 - b_3)}{\sqrt{6}} \times V_{cs}^* \\
A(\Sigma_b^+ \rightarrow Z_{c\pi^+} \Sigma^0) &= \frac{(b_1 - b_2 - b_3)}{\sqrt{2}} \times V_{cs}^* \\
A(\Sigma_b^+ \rightarrow Z_{c\pi^0} \Sigma^+) &= \frac{(-b_1 + b_2 - b_3)}{\sqrt{2}} \times V_{cs}^* \\
A(\Sigma_b^+ \rightarrow Z_{c\eta_8} \Sigma^+) &= \frac{(b_1 + b_2 + b_3)}{\sqrt{6}} \times V_{cs}^* \\
A(\Sigma_b^+ \rightarrow Z_{c\bar{K}^0} p) &= b_1 \times V_{cs}^* \\
A(\Sigma_b^0 \rightarrow Z_{c\pi^+} \Sigma^-) &= \frac{(b_1 - b_2 - b_3)}{\sqrt{2}} \times V_{cs}^* \\
A(\Sigma_b^0 \rightarrow Z_{c\pi^0} \Lambda^0) &= -\frac{(b_1 + b_2 - b_3)}{\sqrt{6}} \times V_{cs}^* \\
A(\Sigma_b^0 \rightarrow Z_{c\pi^-} \Sigma^+) &= \frac{(-b_1 + b_2 + b_3)}{\sqrt{2}} \times V_{cs}^* \\
A(\Sigma_b^0 \rightarrow Z_{c\pi^+} \Sigma^-) &= \frac{(b_1 - b_2 - b_3)}{\sqrt{2}} \times V_{cs}^* \\
A(\Sigma_b^0 \rightarrow Z_{c\pi^0} \Lambda^0) &= \frac{(-b_1 - b_2 - b_3)}{\sqrt{2}} \times V_{cs}^* \\
A(\Sigma_b^0 \rightarrow Z_{c\pi^-} \Sigma^+) &= \frac{(-b_1 + b_2 + b_3)}{\sqrt{2}} \times V_{cs}^* \\
A(\Sigma_b^- \rightarrow Z_{cK^-} p) &= \frac{-b_1}{\sqrt{2}} \times V_{cs}^* \\
A(\Sigma_b^- \rightarrow Z_{c\pi^0} \Sigma^-) &= \frac{(-b_1 + b_2 + b_3)}{\sqrt{2}} \times V_{cs}^* \\
A(\Sigma_b^- \rightarrow Z_{c\pi^-} \Sigma^0) &= \frac{(-b_1 - b_2 - b_3)}{\sqrt{2}} \times V_{cs}^* \\
A(\Sigma_b^- \rightarrow Z_{cK^-} n) &= -b_1 \times V_{cs}^* \\
A(\Sigma_b^- \rightarrow Z_{c\eta_8} \Sigma^-) &= \frac{-(b_1 + b_2 + b_3)}{\sqrt{6}} \times V_{cs}^* \\
A(\Xi_b^0 \rightarrow Z_{c\bar{K}^0} \Sigma^0) &= -\frac{1}{2} (b_2 + b_3) V_{cs}^* \\
A(\Xi_b^0 \rightarrow Z_{c\bar{K}^0} \Lambda^0) &= -\frac{(2b_1 - b_2 + b_3)}{2\sqrt{3}} \times V_{cs}^* \\
A(\Xi_b^0 \rightarrow Z_{cK^-} \Sigma^+) &= \frac{(b_2 + b_3)}{\sqrt{2}} V_{cs}^*
\end{aligned}$$



$$\begin{aligned}
A(\Xi_b^0 \rightarrow Z_{cK} \Lambda^0) &= \frac{(2b_1 - b_2 + b_3)}{2\sqrt{3}} \times V_{cs}^* \\
A(\Xi_b^0 \rightarrow Z_{c\bar{K}^0} \Sigma^-) &= -\frac{(b_2 + b_3)}{\sqrt{2}} \times V_{cs}^* \\
A(\Xi_b^0 \rightarrow Z_{cK} \Sigma^0) &= -\frac{(b_2 + b_3)}{2} V_{cs}^*.
\end{aligned} \tag{3.1.23}$$

Similarly, we can write

$$\begin{aligned}
A(\Sigma_b^+ \rightarrow Z_{c\pi^0} p) &= -\frac{(b_2 + b_3)}{\sqrt{2}} \times V_{cd}^* \\
A(\Sigma_b^+ \rightarrow Z_{cK^+} \Sigma^0) &= -\frac{(b_1 + b_3)}{\sqrt{2}} \times V_{cd}^* \\
A(\Sigma_b^+ \rightarrow Z_{cK^+} \Lambda^0) &= \frac{((-b_1 + b_2 + b_3))}{\sqrt{6}} \times V_{cd}^* \\
A(\Sigma_b^+ \rightarrow Z_{cK^+} \Sigma^+) &= -b_1 \times V_{cd}^* \\
A(\Sigma_b^+ \rightarrow Z_{c\eta_8} p) &= \frac{(2b_1 + b_2 + b_3)}{\sqrt{6}} \times V_{cd}^* \\
A(\Sigma_b^+ \rightarrow Z_{c\pi^+} n) &= -b_2 \times V_{cd}^* \\
A(\Sigma_b^0 \rightarrow Z_{c\pi^0} n) &= \frac{1}{2} (b_2 - b_3) \times V_{cd}^* \\
A(\Sigma_b^0 \rightarrow Z_{c\pi^-} p) &= \frac{1}{\sqrt{2}} (b_2 - b_3) \times V_{cd}^* \\
A(\Sigma_b^0 \rightarrow Z_{cK^0} \Lambda^0) &= \frac{(-b_1 + 2b_2 + b_3)}{2\sqrt{3}} \times V_{cd}^* \\
A(\Sigma_b^0 \rightarrow Z_{cK^0} \Sigma^0) &= \frac{1}{2} (b_2 + b_3) \times V_{cd}^* \\
A(\Sigma_b^0 \rightarrow Z_{c\eta_8} n) &= \frac{(2b_1 - b_2 - b_3)}{2\sqrt{3}} \times V_{cd}^* \\
A(\Sigma_b^0 \rightarrow Z_{cK^+} \Sigma^-) &= \frac{(b_3 - b_1)}{\sqrt{2}} \times V_{cd}^* \\
A(\Sigma_b^- \rightarrow Z_{c\pi^-} n) &= -b_3 \times V_{cd}^* \\
A(\Xi_b^0 \rightarrow Z_{c\pi^0} \Sigma^0) &= \frac{(b_1 + b_2)}{2\sqrt{2}} \times V_{cd}^* \\
A(\Xi_b^0 \rightarrow Z_{c\pi^0} \Lambda^0) &= \frac{(b_1 + b_2 + b_3)}{2\sqrt{6}} \times V_{cd}^* \\
A(\Xi_b^0 \rightarrow Z_{c\pi^-} \Sigma^+) &= \frac{b_1}{\sqrt{2}} \times V_{cd}^*
\end{aligned}$$

$$\begin{aligned}
A(\Xi_b^0 \rightarrow Z_{c\bar{K}^0} n) &= \frac{-b_2}{\sqrt{2}} \times V_{cd}^* \\
A(\Xi_b^0 \rightarrow Z_{cK^-} p) &= \frac{(b_1 - b_2 - b_3)}{\sqrt{2}} \times V_{cd}^* \\
A(\Xi_b^0 \rightarrow Z_{c\eta_8} \Lambda^0) &= -\frac{(b_1 + b_2)}{2\sqrt{2}} \times V_{cd}^* \\
A(\Xi_b^0 \rightarrow Z_{c\eta_8} \Sigma^0) &= \frac{(b_1 + b_2 - 2b_3)}{2\sqrt{6}} \times V_{cd}^* \\
A(\Xi_b^0 \rightarrow Z_{c\pi^+} \Sigma^-) &= \frac{b_2}{\sqrt{2}} \times V_{cd}^* \\
A(\Xi_b^- \rightarrow Z_{c\pi^-} \Sigma^0) &= \frac{1}{2}(b_2 - b_1) \times V_{cd}^* \\
A(\Xi_b^- \rightarrow Z_{cK^-} n) &= \frac{(b_1 - b_3)}{\sqrt{2}} \times V_{cd}^* \\
A(\Xi_b^- \rightarrow Z_{c\pi^0} \Sigma^-) &= \frac{(b_1 - b_3)}{\sqrt{2}} \times V_{cd}^* \\
A(\Xi_b^- \rightarrow Z_{c\eta_8} \Sigma^-) &= \frac{(b_1 - b_3 + b_2)}{\sqrt{2}} \times V_{cd}^* \\
A(\Xi_b^- \rightarrow Z_{c\pi^-} \Lambda^0) &= \frac{(b_1 + b_2 + b_3)}{2\sqrt{3}} \times V_{cd}^* \\
A(\Omega_b^- \rightarrow Z_{cK^-} \Lambda^0) &= \frac{(-2b_1 + b_2 + b_3)}{\sqrt{6}} \times V_{cd}^* \\
A(\Omega_b^- \rightarrow Z_{c\bar{K}^0} \Sigma^-) &= b_2 \times V_{cd}^* \\
A(\Omega_b^- \rightarrow Z_{cK^-} \Sigma^0) &= \frac{1}{\sqrt{2}} b_2 \times V_{cd}^* \tag{3.1.24}
\end{aligned}$$

As we are considering the  $SU(3)$  flavor symmetry, therefore, the particles in the same multiplet have the same mass. Hence, they do not make any difference to the phase space, allowing us to equate the decay rate of the processes with same amplitude for a particular initial state baryon. Hence, the decay rates deduced from the Eqs. (3.1.21) and (3.1.22) are following

$$\Gamma(\Xi_b^- \rightarrow Z_{c\pi^0} \Sigma^-) = \Gamma(\Xi_b^- \rightarrow Z_{c\pi^-} \Sigma^+)$$

$$\begin{aligned}
\Gamma(\Lambda^0 \rightarrow Z_{c\bar{K}^0} n) &= \Gamma(\Lambda^0 \rightarrow Z_{cK^-} p) \\
\Gamma(\Xi_b^0 \rightarrow Z_{c\pi^0} n) &= \frac{1}{2} \Gamma(\Xi^- \rightarrow Z_{c\pi^-} p) \\
\Gamma(\Xi_b^0 \rightarrow Z_{c\pi^+} \Sigma^-) &= \Gamma(\Xi_b^0 \rightarrow Z_{cK^0} n), \Gamma(\Xi_b^0 \rightarrow Z_{c\bar{K}^0} \Lambda^0) = \Gamma(\Xi_b^- \rightarrow Z_{cK^-} \Lambda^0) \\
\Gamma(\Lambda_b^0 \rightarrow Z_{c\pi^+} \Sigma^-) &= \Gamma(\Lambda_b^0 \rightarrow Z_{c\pi^0} \Sigma^0) = \Gamma(\Lambda_b^0 \rightarrow Z_{c\pi^-} \Sigma^+) \\
\Gamma(\Lambda_b^0 \rightarrow Z_{cK^+} \Sigma^-) &= \Gamma(\Lambda_b^0 \rightarrow Z_{cK^0} \Sigma^0) = \Gamma(\Xi_b^0 \rightarrow Z_{cK^-} n) \\
\Gamma(\Xi_b^0 \rightarrow Z_{c\pi^0} \Lambda^0) &= \Gamma(\Xi_b^0 \rightarrow Z_{c\eta_8} \Sigma^0) = \frac{1}{2} \Gamma(\Xi_b^- \rightarrow Z_{c\pi^-} \Lambda^0) = \frac{1}{2} \Gamma(\Xi_b^- \rightarrow Z_{c\eta_8} \Sigma^-) \\
\Gamma(\Xi_b^0 \rightarrow Z_{c\bar{K}^0} \Sigma^0) &= \frac{1}{2} \Gamma(\Xi_b^0 \rightarrow Z_{cK^-} \Sigma^+) = \frac{1}{2} \Gamma(\Xi_b^- \rightarrow Z_{cK^-} \Sigma^0) = \frac{1}{2} \Gamma(\Xi_b^- \rightarrow Z_{c\bar{K}^0} \Sigma^0).
\end{aligned} \tag{3.1.25}$$

Similarly relations evaluated from Eqs.(3.1.23) and (3.1.24) are

$$\begin{aligned}
\Gamma(\Xi_b^0 \rightarrow Z_{c\bar{K}^0} \Lambda^0) &= \Gamma(\Xi_b^- \rightarrow Z_{cK^-} \Lambda^0) \\
\Gamma(\Xi_b^0 \rightarrow Z_{c\eta_8} \Sigma^0) &= \frac{1}{2} \Gamma(\Xi_b^- \rightarrow Z_{c\eta_8} \Sigma^-), \Gamma(\Xi_b^- \rightarrow Z_{c\pi^0} \Sigma^-) = \Gamma(\Xi_b^- \rightarrow Z_{c\pi^-} \Sigma^0) \\
\Gamma(\Sigma^+ \rightarrow Z_{c\pi^0} p) &= \Gamma(\Sigma_b^- \rightarrow Z_{c\pi^-} p), \Gamma(\Sigma^+ \rightarrow Z_{c\pi^0} \Lambda^0) = 2\Gamma(\Sigma_b^- \rightarrow Z_{c\pi^-} p) \\
\Gamma(\Sigma^+ \rightarrow Z_{c\eta_8} p) &= 2\Gamma(\Sigma^0 \rightarrow Z_{c\eta_8} n), \Gamma(\Sigma^- \rightarrow Z_{c\pi^-} n) = \Gamma(\Sigma^- \rightarrow Z_{cK^0} \Sigma^-) \\
\Gamma(\Xi_b^0 \rightarrow Z_{c\pi^0} \Lambda^0) &= \frac{1}{2} \Gamma(\Xi_b^- \rightarrow Z_{c\pi^-} \Lambda^0), \Gamma(\Xi_b^0 \rightarrow Z_{c\pi^+} \Lambda^0) = \Gamma(\Xi_b^0 \rightarrow Z_{c\eta_8} \Lambda^0) \\
\Gamma(\Sigma_b^+ \rightarrow Z_{c\pi^+} \Lambda^0) &= \Gamma(\Sigma_b^0 \rightarrow Z_{c\pi^0} \Lambda^0) = \Gamma(\Sigma_b^- \rightarrow Z_{c\pi^-} \Lambda^0) \\
\Gamma(\Sigma_b^+ \rightarrow Z_{cK^+} \Sigma^0) &= \Gamma(\Sigma_b^0 \rightarrow Z_{cK^+} \Sigma^-) = \Gamma(\Xi_b^0 \rightarrow Z_{c\eta_8} \Sigma^-) \\
\Gamma(\Sigma_b^+ \rightarrow Z_{c\eta_8} \Sigma^+) &= \Gamma(\Sigma_b^0 \rightarrow Z_{c\eta_8} \Sigma^0) = \Gamma(\Sigma_b^- \rightarrow Z_{c\eta_8} \Sigma^-) \\
\Gamma(\Sigma_b^+ \rightarrow Z_{c\bar{K}^0} p) &= \Gamma(\Sigma_b^+ \rightarrow Z_{c\bar{K}^0} n) = \Gamma(\Sigma_b^0 \rightarrow Z_{cK^-} p) = \Gamma(\Sigma_b^- \rightarrow Z_{cK^-} n) \\
\Gamma(\Xi \rightarrow Z_{c\bar{K}^0} \Sigma^0) &= \frac{1}{2} \Gamma(\Xi \rightarrow Z_{cK^-} \Sigma^+) = \Gamma(\Xi \rightarrow Z_{c\bar{K}^0} \Sigma^-) = \Gamma(\Xi \rightarrow Z_{cK^-} \Sigma^0) \\
\Gamma(\Sigma_b^+ \rightarrow Z_{c\pi^+} \Sigma^0) &= \frac{1}{2} \Gamma(\Sigma_b^+ \rightarrow Z_{c\pi^0} \Sigma^+) = \Gamma(\Sigma_b^0 \rightarrow Z_{c\pi^+} \Sigma^-) = \Gamma(\Sigma_b^0 \rightarrow Z_{c\pi^-} \Sigma^+) \\
&= \Gamma(\Sigma_b^- \rightarrow Z_{c\pi^0} \Sigma^-) = \Gamma(\Sigma_b^- \rightarrow Z_{c\pi^-} \Sigma^0)
\end{aligned} \tag{3.1.26}$$

## 3.2 Effective Hamiltonian

The utilization of helicity amplitude approach proves to be quite advantageous when it comes to describing a wide range of observable variables in the context of heavy quark decays. It is well established that integrating out the heavy degree of freedoms from a full theory i.e., top quark,  $W$  and  $Z$  bosons at electroweak scale in the SM, a low energy effective theory can be constructed. The weak effective Lagrangian consist of six-dimensional local operators of the light SM fields (fermions, photons and gluons) suppressed by inverse powers of  $m_W$ . The amplitude  $\mathcal{M}(\Lambda_b^0 \rightarrow \Lambda^0 Z_c^0$  (3900)) is induced by the quark level transition  $b \rightarrow s\bar{c}c$  whose effective Hamiltonian can be written as

$$\mathcal{H}^{eff} = \frac{G_F}{\sqrt{2}} V_{cb} V_{cq}^* (C_1 \mathcal{O}_1 + C_2 \mathcal{O}_2) \quad (3.2.1)$$

where

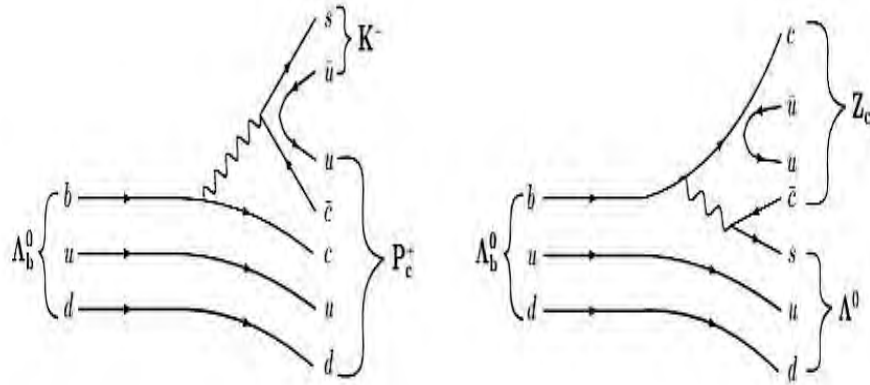
$$\begin{aligned} \mathcal{O}_1 &= (\bar{c}_\alpha (1 - \gamma_5) \gamma_\mu b_\beta) (\bar{q}_\beta (1 - \gamma_5) \gamma_\mu c_\alpha) \\ \mathcal{O}_2 &= (\bar{c}_\alpha (1 - \gamma_5) \gamma_\mu b_\alpha) (\bar{q}_\beta (1 - \gamma_5) \gamma_\mu c_\beta) \end{aligned} \quad (3.2.2)$$

where  $q = d$  or  $s$ ,  $G_F$  is Fermi constant,  $V_{ij}$  are corresponding CKM matrix elements,  $\mathcal{O}_i$  are low-energy effective operators, together with their related Wilson coefficients  $C_i$ , are obtained through the process of integrating out high-energy contributions.

## 3.3 Helicity amplitudes and Form Factors for $\Lambda_b \rightarrow \Lambda$ transitions

In  $\Lambda_b \rightarrow \Lambda$  transition, the matrix elements different currents are parameterized in terms of Form Factors. Helicity formalism provide useful way to describe these transitions. The amplitude is

$$\mathcal{M}(\Lambda_b^0 \rightarrow \Lambda^0 Z_c^0$$
 (3900)) =  $\frac{G_F}{\sqrt{2}} V_{cb} V_{cq}^* a_2 f_{Z_c} M_{Z_c} H^j(s_{\Lambda_b}, s_\Lambda, s_{Z_c})$  (3.3.1)


 Figure 3.3.1: Feynman diagrams for the  $\Lambda_b^0 \rightarrow K^- P_c^+$  and for the  $\Lambda_b^0 \rightarrow \Lambda^0 Z_c^0$  [57]

where  $a_2 = C_1 + C_2/N_c$ ,  $C_1 = -0.248$  and  $C_2 = 1.107$  [47, 48],  $f_{Z_c} = 0.0051$  GeV [49] is the decay constant and  $M_{Z_c} = 3.901$  MeV [50] are the mass of  $Z_c^0$  (3900).

The helicity amplitudes  $H^j(s_1, s_2)$  with  $j$  for different currents, i.e., vector ( $V$ ) or axial-vector ( $A$ ) are given as [51]:

$$\begin{aligned} H^V(s_{\Lambda_b}, s_\Lambda, s_{Z_c}) &\equiv \epsilon^{\mu*}(s_{Z_c}) \langle \Lambda(k_\Lambda, s_\Lambda) | \bar{s} \gamma_\mu b | \Lambda_b(p_{\Lambda_b}, s_{\Lambda_b}) \rangle, \\ H^A(s_{\Lambda_b}, s_\Lambda, s_{Z_c}) &\equiv \epsilon^{\mu*}(s_{Z_c}) \langle \Lambda(k_\Lambda, s_\Lambda) | \bar{s} \gamma_\mu \gamma_5 b | \Lambda_b(p_{\Lambda_b}, s_{\Lambda_b}) \rangle, \end{aligned} \quad (3.3.2)$$

In component form, the matrix element can be described using weak transition form factors

$$\langle \Lambda(k_\Lambda, s_\Lambda) | \bar{s} \gamma^\mu b | \Lambda_b(p_{\Lambda_b}, s_{\Lambda_b}) \rangle = \bar{u}(k_\Lambda, s_\Lambda) \left( \gamma^\mu f_1 + \frac{p_{\Lambda_b}^\mu}{m_{\Lambda_b}} f_2 + \frac{k_\Lambda^\mu}{m_\Lambda} f_3 \right) u(p_{\Lambda_b}, s_{\Lambda_b}), \quad (3.3.3)$$

$$\langle \Lambda(k_\Lambda, s_\Lambda) | \bar{s} \gamma_\mu \gamma_5 b | \Lambda_b(p_{\Lambda_b}, s_{\Lambda_b}) \rangle = \bar{u}(k_\Lambda, s_\Lambda) \left( \gamma^\mu g_1 + \frac{p_{\Lambda_b}^\mu}{m_{\Lambda_b}} g_2 + \frac{k_\Lambda^\mu}{m_\Lambda} g_3 \right) u(p_{\Lambda_b}, s_{\Lambda_b}), \quad (3.3.4)$$

Here  $s_{\Lambda_b}(p_{\Lambda_b})$  and  $s_\Lambda(k_\Lambda)$  are the spin and momenta of parent baryon ( $\Lambda_b$ ) and daughter baryon  $\Lambda$ , respectively. The non-perturbative quantities i.e., FFs, need to be calculated in some model.  $\Lambda_b \rightarrow \Lambda$  Helicity amplitudes are examined in the context of the complete quark model wave function (MCN) to investigate the form factors as [52]

$$f(q^2) = (a_0 + a_2 p_\Lambda^2 + a_4 p_\Lambda^4) \exp \left( - \frac{6m_q^2 p_\Lambda^2}{2\tilde{m}_\Lambda^2 (\alpha_{\Lambda_b^0}^2 + \alpha_\Lambda^2)} \right) \quad (3.3.5)$$

Table 3.3.1: Input parameters for spin-1/2 baryon  $\Lambda$  in MCN quark model. [53]

$\Lambda^0$			
form factor	$a_0$	$a_2$	$a_4$
$f_1^+$	1.21	0.319	-0.0177
$f_2^+$	-0.202	-0.219	-0.0103
$f_3^+$	-0.0615	0.0102	-0.00139
$g_1^+$	0.927	0.104	-0.00552
$g_2^+$	-0.236	-0.233	0.011
$g_3^+$	0.0756	0.0195	-0.00115
$\alpha_\Lambda = 0.387$		$\alpha_{\Lambda_b} = 0.443$	

$$p_\Lambda = \frac{m_{\Lambda_b}^0}{2} \left[ \left( 1 - \frac{m_\Lambda^2}{m_{\Lambda_b}^2} \right)^2 - 2 \left( 1 + \frac{m_\Lambda^2}{m_{\Lambda_b}^2} \right) \frac{q^2}{m_{\Lambda_b}^2} + \left( \frac{q^2}{m_{\Lambda_b}^2} \right)^2 \right]. \quad (3.3.6)$$

with  $\tilde{m} = m_u + m_d + m_s$ . The values for FF's are given in table [2].

### 3.4 Kinematics of Hadronic part

In  $\Lambda_b$  rest frame, the momentum of  $\Lambda$  and  $Z_c$  is define as

$$\begin{aligned} p_{\Lambda_b}^\mu &= (m_{\Lambda_b}, 0, 0, 0) \\ k_\Lambda^\mu &= (E_\Lambda, 0, 0, -|\vec{q}|) \\ q^\mu &= (m_{\Lambda_b} - E_\Lambda, 0, 0, +|\vec{q}|), \end{aligned} \quad (3.4.1)$$

Lets define

$$s_\pm \equiv (m_{\Lambda_b} \pm m_\Lambda)^2 - q^2 \quad \text{and} \quad s \equiv q^2.$$

The polarization vectors of the  $Z_c$  are written as

$$\begin{aligned} \epsilon^\mu(t) &= \frac{1}{\sqrt{s}}(q_0, 0, 0, |\vec{q}|) \\ \epsilon^\mu(0) &= \frac{1}{s}(|\vec{q}|, 0, 0, q_0) \\ \epsilon^\mu(\pm) &= \frac{1}{\sqrt{2}}(0, \mp 1, -i, 0), \end{aligned} \quad (3.4.2)$$

The spinor for  $\Lambda_b \rightarrow \Lambda$  case are constructed with the help of four vectors defined above in

$\Lambda_b$ -rest frame

$$u(p, s) = \frac{\not{p} + m}{\sqrt{p_0 + m}} \begin{pmatrix} \chi^{(s)} \\ 0 \end{pmatrix}$$

$$\bar{u}_2 \left( \pm \frac{1}{2}, p_2 \right) = \sqrt{E_2 - M_2} \begin{pmatrix} \chi_{\pm}^\dagger & \frac{\mp |\vec{q}|}{E_2 + M_2} \chi_{\pm}^\dagger \end{pmatrix}$$

$$u_1 \left( \pm \frac{1}{2}, p_1 \right) = \sqrt{2M_1} \begin{pmatrix} \chi_{\pm} \\ 0 \\ 0 \end{pmatrix}$$

$$\bar{u}_1 \left( \pm \frac{1}{2}, p_1 \right) = \sqrt{2M_1} \begin{pmatrix} \chi_{\pm}^\dagger & 0 & 0 \end{pmatrix}$$

$$u_2 \left( \pm \frac{1}{2}, p_2 \right) = \sqrt{E_2 - M_2} \begin{pmatrix} \chi_{\pm} \\ \frac{\mp |\vec{q}|}{E_2 + M_2} \chi_{\pm} \end{pmatrix}, \quad (3.4.3)$$

$$\chi_+ = \begin{pmatrix} 1 \\ 0 \end{pmatrix}, \chi_- = \begin{pmatrix} 0 \\ 1 \end{pmatrix}, \quad (3.4.4)$$

with

$$\begin{aligned} \chi^{+\frac{1}{2}} &= \begin{pmatrix} \cos \left( \frac{\theta}{2} \right) \\ \sin \left( \frac{\theta}{2} \right) e^{i\phi} \end{pmatrix}, & \chi^{-\frac{1}{2}} &= \begin{pmatrix} -\sin \left( \frac{\theta}{2} \right) e^{i\phi} \\ \cos \left( \frac{\theta}{2} \right) \end{pmatrix}, \\ \eta^{+\frac{1}{2}} &= \chi^{-\frac{1}{2}}, & \eta^{-\frac{1}{2}} &= -\chi^{+\frac{1}{2}} \end{aligned} \quad (3.4.5)$$

### 3.5 Hadronic Helicity amplitudes

Using the spinor matrix elements for given combination of spin orientation in Eq. (3.4.5),

we get the following helicity amplitude in terms of  $\Lambda_b \rightarrow \Lambda$  transition FFs [50]:

$$\begin{aligned}
 H_1^V \left( +\frac{1}{2}, +\frac{1}{2}, 0 \right) &= H^V \left( -\frac{1}{2}, -\frac{1}{2}, 0 \right) = \sqrt{\frac{s_-}{s}} \left[ (m_{\Lambda_b} + m_{\Lambda}) f_1(s) - \frac{s}{m_{\Lambda_b}} f_2(s) \right], \\
 H_2^V \left( -\frac{1}{2}, +\frac{1}{2}, 1 \right) &= H^V \left( +\frac{1}{2}, -\frac{1}{2}, -1 \right) = \sqrt{2s_-} \left[ f_1(s) - \frac{m_{\Lambda_b} + m_{\Lambda}}{m_{\Lambda_b}} f_2(s) \right], \\
 H_1^A \left( +\frac{1}{2}, +\frac{1}{2}, 0 \right) &= -H^A \left( -\frac{1}{2}, -\frac{1}{2}, 0 \right) = \sqrt{\frac{s_+}{s}} \left[ (m_{\Lambda_b} - m_{\Lambda}) g_1(s) + \frac{s}{m_{\Lambda_b}} g_2(s) \right], \\
 H_2^A \left( -\frac{1}{2}, +\frac{1}{2}, 1 \right) &= -H^A \left( +\frac{1}{2}, -\frac{1}{2}, -1 \right) = \sqrt{2s_+} \left[ g_1(s) + \frac{m_{\Lambda_b} - m_{\Lambda}}{m_{\Lambda_b}} g_2(s) \right]. \quad (3.5.1)
 \end{aligned}$$

One can write the total helicity amplitude as  $H = H^V - H^A$ . By using all above parameters, after the two body phase space integration by using Mathematica 12.1, we get the following expression of the decay width

$$\Gamma(\Lambda_b^0 \rightarrow \Lambda^0 Z_c^0(3900)) = \sum_{s_{\Lambda_b^0}, s_{\Lambda}} \frac{|\bar{p}_{\Lambda}|}{8\pi m_{\Lambda_b^0}^2} \frac{1}{2} |\mathcal{M}(\Lambda_b^0 \rightarrow \Lambda^0 Z_c^0(3900))|^2. \quad (3.5.2)$$

By putting all the Helicity amplitudes in the Eq. (3.5.2) and performing sum over all the Helicity amplitudes, we get following expression

$$\Gamma(\Lambda_b^0 \rightarrow \Lambda^0 Z_c^0(3900)) = \frac{|\bar{p}_{\Lambda}|}{8\pi m_{\Lambda_b^0}^2} \frac{1}{2} |H_1^V + H_2^V + H_1^A + H_2^A|^2. \quad (3.5.3)$$

Using Eq. (3.3.1), in the above expression, we get the following expression

$$= \sum_{s_{\Lambda_b^0}, s_{\Lambda}} \frac{|\bar{p}_{\Lambda}|}{8\pi m_{\Lambda_b^0}^2} \left| \frac{G_F}{\sqrt{2}} V_{cb} V_{cq}^* a_2 f_{Z_c} M_{Z_c} H^j(s_{\Lambda_b}, s_{\Lambda}, s_{Z_c}) \right|^2, \quad (3.5.4)$$

and after inserting numerical inputs in the above expression, we get the following numerical values with the help of Mathematica 12.1

$$\Gamma(\Lambda_b^0 \rightarrow \Lambda^0 Z_c^0(3900)) = 8.61 \times 10^{-20} \text{GeV}.$$

The corresponding branching ratio comes to be of the order of  $10^{-7}$ , while the exact calculated



Decays	decay rates
$\Gamma(\Xi_b^- \rightarrow Z_{c\pi^0}\Sigma^-)$	$8.40 \times 10^{-21}$
$\Gamma(\Xi_b^- \rightarrow Z_{c\pi^-}\Sigma^0)$	$8.40 \times 10^{-21}$

Table 3.5.1: Decay rates

decays	decay rates( $GeV$ )
$\Xi_b^0 \rightarrow Z_{c\pi^0}\Lambda^0$	$2.64 \times 10^{-21}$
$\Xi_b^0 \rightarrow Z_{c\eta_8}\Sigma^0$	$2.64 \times 10^{-21}$
$\Xi_b^- \rightarrow Z_{c\pi^-}\Lambda^0$	$2 \times 2.64 \times 10^{-21}$
$\Xi_b^- \rightarrow Z_{c\eta_8}\Sigma^-$	$2 \times 2.64 \times 10^{-21}$

Table 3.5.2: Decay rates

value is

$$\mathcal{B}(\Lambda_b^0 \rightarrow \Lambda^0 Z_c^0(3900)) = 1.93 \times 10^{-7}.$$

Similarly, one obtains the estimation of partial decay widths and branching fractions

$$\Gamma(\Xi_b^- \rightarrow \Sigma^- Z_c^0(3900)) = 8.40 \times 10^{-21} GeV, \Gamma(\Xi_b^0 \rightarrow \Lambda^0 Z_c^0(3900)) = 2.64 \times 10^{-21} GeV,$$

$$\mathcal{B}(\Xi_b^- \rightarrow \Sigma^- Z_c^0(3900)) = 2.01 \times 10^{-8}, \mathcal{B}(\Xi_b^0 \rightarrow \Lambda^0 Z_c^0(3900)) = 5.94 \times 10^{-8}.$$

The calculation of branching fractions for the decay of b-baryons, where the tetraquark is present in the final states, is as follows for various channels. For  $\Xi_b^- \rightarrow \Sigma^- Z_c^0$ , the branching ratio is  $2.01 \times 10^{-8}$ . Similarly for  $\Xi_b^- \rightarrow \Lambda^0 Z_c$  has the branching ratio value  $1.26 \times 10^{-8}$ .  $\Xi_b^0 \rightarrow \Lambda^0 Z_c$  has the branching ratio  $5.94 \times 10^{-8}$ .  $\Lambda_b^0 \rightarrow \Lambda^0 Z_c^0$  has the branching ratio  $1.93 \times 10^{-8}$ .  $\Xi_b^0 \rightarrow \Sigma^0 Z_c^-$  has the value  $2.01 \times 10^{-8}$ .  $\Xi_b^- \rightarrow \Sigma^- Z_{c\eta_8}^-$  has the branching ratio value  $1.26 \times 10^{-8}$ . Similarly,  $\Xi_b^0 \rightarrow \Sigma^0 Z_{c\eta_8}^-$  has the value  $5.94 \times 10^{-9}$ .

From above table

$$\Gamma(\Xi_b^- \rightarrow Z_{c\pi^0}\Sigma^-) = \Gamma(\Xi_b^- \rightarrow Z_{c\pi^-}\Sigma^0).$$

which is in best match with the experimental measurements. According to the measured results of BESIII, the cascade decay form of this transition is  $\Lambda_b^0 \rightarrow \Lambda^0 Z_c^0(3900) \rightarrow pJ/\rho\pi^-\pi^+$ . If  $\Lambda_b$  particle is replaced with the ( $\Xi$ ) cascade particle then the branching fraction's magnitude would be small due to  $\left|\frac{V_{cs}^*}{V_{cd}^*}\right|^2$  as it will serve as suppression factor. As amplitudes here are represented in the SU(3) symmetry so this symmetry is best to find the

exotic states like  $Z_0$ .

# Chapter 4

## Results And Discussion

In this dissertation we have worked in the Helicity formalism to express the decay rate of  $b$ -baryon decay  $\Lambda_b \rightarrow \Lambda^0 Z^0$  (3900) in the SM. The main advantage of the helicity formalism is that any observables of the problem can be expressed in terms of bi-linear forms of hadronic helicity matrix. The numerical results obtained for  $\Lambda_b \rightarrow \Lambda$  transitions are defined in chapter 3. As experimentally, exotic states of  $Z_0$  have been observed by LHCb, several works are being performed in search of more modes of these states and for this purpose,  $b \rightarrow s$  transitions have been of profound help. Decay amplitudes are parametrized in SU(3) 's representations that are irreducible. In this dissertation, we have reviewed the calculation for the decay width of  $\Lambda_b^0 \rightarrow \Lambda^0 Z_c^0$  (3900) that helps in the estimation of the partial decay width of  $b$ -baryons. Weak decay of  $b$ -baryon to exotic states and lighter baryon is studied with greater details. By using Helicity amplitude technique, partial decay widths are calculated to get more information about tetraquarks. However, four quarks forming the bound states could not be studied since we don't have any perfect landscape for quark states. Moreover, it is expected in future to be found as LHCb has found the pentaquarks too. Form factors used in the calculation have been taken from MCN model and the remaining results are calculated by the use of Mathematica 12.1 and the numerical values obtained came to be in perfect match with the experimental results as the partial decay width is  $8.61 \times 10^{-20} \text{ GeV}$  and the estimated branching fraction is of the order of the magnitude  $10^{-7}$  for the transition  $\Lambda_b^0 \rightarrow \Lambda^0 Z_c^0$  (3900). This motivates the exploration of  $Z_c^0$  properties and production mechanisms through weak decays of  $b$ -baryons like the  $\Lambda_b^0$ . Our research findings not only demonstrate the success of our

theoretical framework but also contribute to the understanding of hadronic matter and the exploration of exotic hadronic states. The agreement with experimental results highlights the importance of future investigations in this field, which could provide further insights into the nature of these elusive particles and advance our knowledge of the fundamental constituents of matter.

# Bibliography

- [1] A.Salam, Conf.Proc. C **680519** (1968),367-377.
- [2] G.Aad et al. Physics. Rev. Lett., 114, (2015) 191803.
- [3] [ATLAS, CDF, CMS and DO], (2014) ArXive :1403.4427 [hep-ex].
- [4] U. Husemann, Prog. Part. Nucl. Phys. 95 (2017) 48.
- [5] M. Ablikim et al. [BESIII], Phys. Rev. Lett. 115, no.11, 112003 (2015)  
doi:10.1103/PhysRevLett.115.112003 [arXiv:1506.06018 [hep-ex]]
- [6] R. Aaij et al. [LHCb], Phys. Rev. Lett. 115, 072001 (2015)  
doi:10.1103/PhysRevLett.115.072001 [arXiv:1507.03414 [hep-ex]].
- [7] M. J. Savage and M. B. Wise, Phys. Rev. D 39, 3346 (1989) Erratum: [Phys. Rev. D 40, 3127 (1989)]. doi:10.1103/PhysRevD.39.3346, 10.1103/PhysRevD.40.3127
- [8] G. Arnison et al.[UA1],phys. Lett. B **126** (1983),398.
- [9] P. Bagnaia et al.[UA2], Phys. Lett. B **129** (1983),130.
- [10] G. Aad et al. [ATLAS Collaboration]. 2012 [arXiv:1207.7214v2].
- [11] I. by Sandbox Studio Chicago, “The Standard Model of Particle Physics.  
[http://www.symmetrymagazine.org/standard-model/.](http://www.symmetrymagazine.org/standard-model/)” September, 2021.
- [12] A. Ali, T. Morozumi, Phys. Lett. B **273**, 505(1991).
- [13] S. L. Glashow,Nucl.Phys.**22** (1961),579,588.

- [14] A.Salam, Conf.Proc. C **680519** (1968),367-377.
- [15] P. W. Higgs, Phys. Rev. Lett. **13** (1964) 508.
- [16] M. Gremm, A. Kapustin, Phys. Rev. D 55 (1997) 6924.
- [17] M. Jezabek, L. Motyka, Nucl. Phys. B 501 (1997) 207.
- [18] S. Balk, J.G. Körner, D. Pirjol, K. Schilcher, Z. Phys. C 64 (1994) 37–44.
- [19] Z. Maki, M. Nakagawa and S. Sakata, Prog. Theor. Phys. **28** (1962) 870.
- [20] A. Celis, M. Jung, X.Q. Li, A. Pich, arXiv:1612.07757 [hep-ph].
- [21] R. Klein, T. Mannel, F. Shahriaran, D. van Dyk, Phys. Rev. D 91 (2015) 094034.
- [22] M .S Chanowitz, M. Furman and I. Hinchliffe, Nucl. Phys. B **159** (1979) 225.
- [23] P . Breitenlohner and D. Maison, Commun. Math. Phys. **52** (1977) 11.
- [24] Gerard't Hooft, M.J.G Veltman, Nucl. Phys. B **44** (1972) 189.
- [25] K. G. Wilson, Phys. Rev. **179** (1969), 1499-1512.
- [26] M. Kobayashi and T. Maskawa, Prog. Theor. Phys. **49** (1973) 652.
- [27] F . Abe et al., Phys. Rev. Lett. **81** (1998) 2432[hep-ex/9805034].
- [28] A. Abulencia et al.,Phys. Rev. Lett. **96** (2006) 082002.
- [29] R. Aajj et al.,Phys. Rev. D **95** (2017) no.3, 032005.
- [30] K. A Olive et al. [Heavy Flavor Averaging Group (HFAG)], arXiv:1412.7515[hep-ex].
- [31] R. Aajj et al.,Nature Phys. Rev. **11** (2015) 743.
- [32] S. L Glashow, J lliopoulos and L.Maiani, Phys. Rev. D **2** (1970) 1285.
- [33] V. Khachatryan et al., Nature **522** (2015) 68.
- [34] J.A. Ernst, UMI-95-30386.

- [35] R. Aaij et al., Phys. Lett. B **694** (2010) 209.
- [36] C. Bourrely, I. Caprini and L. Lellouch, Phys. Rev. D **79** (2009) 013008 Erratum : [Phys Rev. D **82** (2010)099902].
- [37] R. Aaij et al., Phys. JHEP **1706** (2017) 108.
- [38] R. Aaij et al., JHEP **1307** (2013) 084.
- [39] R. Aaij et al., JHEP **1406** (2014) 133.
- [40] T. A. Aaltonen et al., Phys. Rev. Lett. **89** (2014) no.7, 072014 .
- [41] R. Aaij et al., Phys. Rev. D. **89** (2014) no.3, 032001.
- [42] R. Aaij et al., Phys. Rev. Lett. **112** (2014) 202001.
- [43] R. Aaij et al., JHEP **07** (2014) ,103.
- [44] M. Ablikim et al. [BESIII], Phys. Rev. Lett. 110, 252001 (2013) doi:10.1103/PhysRevLett.110.252001 [arXiv:1303.5949 [hep-ex]].
- [45] Z. Q. Liu et al. [Belle], Phys. Rev. Lett. 110, 252002 (2013) [erratum: Phys. Rev. Lett. 111, 019901 (2013)] doi:10.1103/PhysRevLett.110.252002 [arXiv:1304.0121 [hep-ex]]
- [46] T. Xiao, S. Dobbs, A. Tomaradze and K. K. Seth, Phys. Lett. B 727, 366-370 (2013) doi:10.1016/j.physletb.2013.10.041 [arXiv:1304.3036 [hep-ex]].
- [47] G. Buchalla, A. J. Buras and M. E. Lautenbacher, Rev. Mod. Phys. 68, 1125-1144 (1996)doi:10.1103/RevModPhys.68.1125 [arXiv:hep-ph/9512380 [hep-ph]].
- [48] Y. m. Wang, Y. Li and C. D. Lu, Eur. Phys. J. C 59, 861-882 (2009) doi:10.1140/epjc/s10052-008- 0846-5 [arXiv:0804.0648 [hep-ph]].
- [49] Z. G. Wang and T. Huang, Phys. Rev. D 89, no.5, 054019 (2014) doi:10.1103/PhysRevD.89.054019 [arXiv:1310.2422 [hep-ph]].
- [50] S. S. Agaev, K. Azizi and H. Sundu, Phys. Rev. D 96, no.3, 034026 (2017) doi:10.1103/PhysRevD.96.034026 [arXiv:1706.01216 [hep-ph]].

- [51] P. Boer, T. fledmann and D. Van Dyk, JHEP 1501 (2015) 155.
- [52] L. Mott and W. Roberts, Int. J. Mod. Phys. A 27, 1250016 (2012)  
doi:10.1142/S0217751X12500169 [arXiv:1108.6129 [nucl-th]].
- [53] Huang, Fei and Xing, Ye and Xu, Ji, Eur. Phys. J. C, 82, 11, 1075, 2022.
- [54] P. Boer, T. fledmann and D. Van Dyk, JHEP **1501** (2015) 155.
- [55] [https://www.researchgate.net/figure/The-left-picture-shows-the-baryon-octet-and-the-right-picture-the-baryon-decuplet\\_fig3\\_238756004](https://www.researchgate.net/figure/The-left-picture-shows-the-baryon-octet-and-the-right-picture-the-baryon-decuplet_fig3_238756004)
- [56] Huang, F., Xing, Y. & Xu, J. Searching for tetraquark through weak decays of b-baryons. Eur. Phys. J. C 82, 1075 (2022). <https://doi.org/10.1140/epjc/s10052-022-11012-6>
- [57] Huang, F., Xing, Y. & Xu, J. Searching for tetraquark through weak decays of b-baryons. Eur. Phys. J. C 82, 1075 (2022). <https://doi.org/10.1140/epjc/s10052-022-11012-6>



# Appendix A

## Dirac Spinor Representation

One has to define the Dirac spinors in term of helicity operator's eigenstate for the calculation of helicity amplitude for  $\Lambda_b^0 \rightarrow \Lambda^0 Z^0(3900)$  decay.

$$u(p, s) = \frac{\not{p} + m}{\sqrt{p_0 + m}} \begin{pmatrix} \chi^{(s)} \\ 0 \end{pmatrix}$$

with

$$\chi^{+\frac{1}{2}} = \begin{pmatrix} \cos\left(\frac{\theta}{2}\right) \\ \sin\left(\frac{\theta}{2}\right) e^{i\phi} \end{pmatrix}, \quad \chi^{-\frac{1}{2}} = \begin{pmatrix} -\sin\left(\frac{\theta}{2}\right) e^{i\phi} \\ \cos\left(\frac{\theta}{2}\right) \end{pmatrix},$$

The spinor for  $\Lambda_b \rightarrow \Lambda$  case are constructed with the help of four vectors defined in section [put section number] in  $\Lambda_b$ -rest frame. The non-zero components for the  $\Lambda_b \rightarrow \Lambda$  transition with the vector or axial vector currents. [54]

$$\bar{u}\left(k_\Lambda, \pm\frac{1}{2}\right) \gamma^\mu u\left(p_{\Lambda_b}, \pm\frac{1}{2}\right) = (\sqrt{s_+}, 0, 0, \sqrt{s_-}),$$

$$\bar{u}\left(k_\Lambda, \pm\frac{1}{2}\right) \gamma^\mu \gamma_5 u\left(p_{\Lambda_b}, \pm\frac{1}{2}\right) = \pm(\sqrt{s_-}, 0, 0, \sqrt{s_+}),$$

and

$$\bar{u}\left(k_\Lambda, \pm\frac{1}{2}\right) \gamma^\mu u\left(p_{\Lambda_b}, \mp\frac{1}{2}\right) = \sqrt{2s_-} \epsilon^\mu(\pm),$$

$$\bar{u}\left(k_\Lambda, \pm\frac{1}{2}\right) \gamma^\mu \gamma_5 u\left(p_{\Lambda_b}, \mp\frac{1}{2}\right) = \mp\sqrt{2s_+} \epsilon^\mu(\pm),$$